Authors response–reviewer 1:

We thank the reviewer for the feedback given. Please see below for a point-to-point response.

albedo can be only used, scientifically speaking, as a proxy of melt extent and melt amount. Not as proxy of ice discharge (as shown by the authors) and not as proxy of summer SMB (also in part driven by summer snowfall anomalies, as also mentioned by the authors). Due to the delay between production of meltwater (highly correlated with albedo I agree) and runoff (depending of the snowpack meltwater retention), runoff not be correlated with albedo at the monthly time scale. Using MAR outputs, at the summer time scale, it is true that MJJA SMB is correlated at -0.96 (-0.88 over 1980-1999) with runoff and 0.66 with snowfall over 1980-2015. But in May for example, SMB is correlated at 0.98 with snowfall and -0.13 with runoff, showing well that albedo cannot be used as proxy of monthly SMB, although MAR is not "the true".

The reviewer is correct in that snowfall impacts MAR SMB variably, and substantially during the early summer (May). However, MAR model results equally suggest that the impact of May SMB on the overall summer-summed (MJJA) SMB is small, as the mean ice sheet SMB in May is on the order of ~5 Gt, in comparison to the -50…-200 Gt seen in the MJJA sums. Thus, we maintain that while the use of the proxy method to attempt to estimate any single month's SMB is indeed an uncertain venture and cannot be recommended, the proxy method can be useful in its original intended use: to test, on observational basis, whether or not runoff is indeed the dominant driver of the whole summer's summed SMB variability.

In consideration of the reviewer's feedback, we propose to revise the manuscript text in sections 1, 2.7.4., and 3.3 to further clarify and emphasize the intended use of the proxy determination as a test case for runoff dominance at the whole summer scale, to caution the reader against using the proxy to attempt inversion of ice sheet SMB for any single summer month, and to relegate the regression equations to supplementary material to further discourage their careless use.

The albedo data was not used as a proxy for ice discharge in any part of the manuscript. Temporal lag correlation analysis was performed for independent (seasonal) estimates of ice discharge and albedo, as a proxy for meltwater production. However, with regard to the comments here and from the other reviewer, we have removed the time-lag analysis with its associated result figure from the manuscript.

- the role of the albedo decrease and the bare ice expansion to the recent melt increase has already been shown a lot of time in previous publications (e.g. Box et al., 2013).

The reviewer appears to refer to this publication: Greenland ice sheet albedo feedback: thermodynamics and atmospheric drivers, Box et al., 2012. These results, and nearly all others present in literature, are obtained from various versions of the MODIS data record and thus covering 2000->. Recent recalibrations of the MODIS instruments have resulted in a significant update of the referred-to findings (Casey et al., 2017), which the CLARA record is now quite consistent with. Also, as mentioned, this is the first study to leverage the full 1982-2015 coverage in CLARA-A2 albedo, based on intercalibrated AVHRR observations whose stability we demonstrate in the manuscript.

The results also clearly indicate that the significance of albedo trends along the GrIS margins is affected by the length of the observational record being investigated; using CLARA allows us to see the relatively stable 1980s-mid-1990s period, which place the subsequent changes during the MODIS era in larger temporal context. The manuscript is not a simple replication of past investigations, but rather seeks to extend the viewpoint and contribute to the ongoing discussion.

- the correlation between GBI and melt (approximated with albedo here) is also some-thing which is known from a long time (see the Hanna et al.,….).

The connection between albedo changes and GBI was presented as part of the discussion and not results precisely because it is intended as supporting evidence for what is revealed in the full CLARA period, also for the pre-MODIS era. The discussion around this point has been revised and expanded to provide further viewpoints into the consistency of the albedo decrease with changes in atmospheric circulation.

- the discussion about the cloud cover seem to be out of the purpose of this paper...and using MAR for this is certainly not a robust basis of validation.

MAR cloud cover is not intended as a validation basis for the satellite record, the comparison is presented to highlight the differences between observations and model, and in the context of commentary regarding other recent progress in the field. Cloud cover and cloud optical properties are highly relevant to surface melt and thus albedo changes, the authors do not quite see why their inclusion into the discussion section would be out of purpose.

To conclude, the authors try to correlate their "new" data with several previous stud-ies/estimates but there is no new interesting scientific message in this paper deserving to accept this paper in TC. However, using this new satellite product deserves to be published, but I recommend to the authors to limit their correlations/comparisons to melt extent (from satellite) or modelled melt amount (as model validation data set). A comparison with the albedo/bare ice extent MODIS based product (notably used as bare ice albedo in RACMO/HIRHAM) will also be more interesting.

The authors disagree with the reviewer on the lack of novelty value in the manuscript. We show that:

1) albedo changes are significantly negative along many parts of the ice sheet margins, are consistent with MODIS for the overlap, display substantial regional variability in the pre-MODIS era, and are consistent with a variety of atmospheric circulation, air temperature, and cloudiness drivers,
2) bare ice extent has most likely expanded and reaches further up the ice sheet,
3) snowfall and atmospheric regime anomalies are potentially strong inhibitors of enhanced surface melt,
4) the year-to-year albedo changes and discharge changes are not strongly connected, supporting recent modeling findings.

Finally, the runoff-dominance test for summer GrIS SMB is the final new piece of information offered.

The reviewer's suggestion to focus on melt extent/amount determination is naturally worthwhile as well, but publications in said fields do already exist for the more commonly used microwave observations (Mernild et al,

2011; Välisuo et al, 2018). Extension to the optical domain is certainly possible, but requiring and deserving a separate study in the authors' view.

Authors response–reviewer Jason Box

on comments: a.) io = “instead of” b.) Comments refer to page then line numberusing X Y

General Remark The study has a lot of value by presenting an expanded (in timeand process) treatment of AVHRR albedo over Greenland. The article makes several major analyses, the fourth of w hich I am not sure should be kept because of its very w idescope, complexity and limited finding.

Thank you for a carefully considered and thorough review. Please see below for our point by point responses. Some typos and unclear expressions w ere also corrected at the authors’ ow n initiative. All page numbers refer to revised manuscript.

Major critique
A.) The fourth major analysis should be more clearly explained or removed*, that w ith lag analysis, basin scale examination of hypothetical meltw ater lubrication of ice dynamics. The study already has a lot of substance. Adding the lagged result only to confirm earlier studies is a bit much.
12 9-16 reinforces that the study is taking the empirical albedo relation too far.
1 24-27 recommend removing this part of the study as it does not directly examine melt-induced flow acceleration w hile much has been evaluated more directly on this topic. See SWIPA 2017chapter 6 https://w ww.amap.no/documents/doc/snow -w ater-ice-and-permafrost-in-the-arctic-sw ipa-2017/1610

In line w ith the feedback here and from the other review er, this analysis has been removed from the manuscript.

7 6-11 difficult to follow

Paragraph removed w ith the albedo-discharge time lag analysis.

B.) Discussion of this study vs Stroeve (2001) Stroeve, J.: Assessment of Greenlandalbedo variability from the advanced very high resolution radiometer Polar Pathfinderdata set, J. Geophys. Res.-Atmos., 106, 33989–34006, doi:10.1029/2001jd900072,2001. How does this study square w ith Stroeve (2001, see Fig 4 etc) w ho found de-creasing trends 1981-1998?
8 29 “majority of the albedo decrease signal originates after 2000” but Stroeve 2001 found a decrease before 2000

Stroeve (2001) pointed out that the negative albedo trends detected (at a set of grid points) w ere not statistically significant and they w ere largely driven by the anomalously low albedos detected during the summer of 1998. We agree that 1998 w as a low -albedo year (see below for CLARA-A2 July monthly mean albedos for 1997-1999), but 1999 w as not, therefore the finding by Stroeve might have been different if the follow ing year had been included in the data. Also, our trends are based on the Theil-Sen trend estimator, w hich is by design robust against outlier influence in the data.

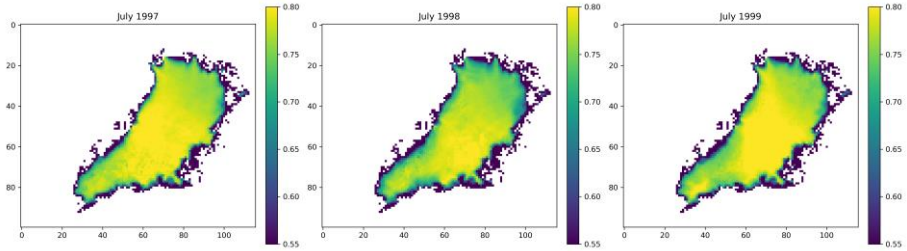

Furthermore, as Polar Pathfinder provides the blue-sky albedo, its seasonal/annual variability is also driven by variability in cloudiness and the cloud radiative properties. Also, the intercalibrations of (earlier) Pathfinder and CLARA-A2 are based on different methods, with the CLARA-A2 method (based on Heidinger et al., 2010) arguably more sophisticated as it leverages the high MODIS calibration as well as stable natural targets. Finally, the Polar Pathfinder dataset only contained data from the afternoon AVHRR satellites, meaning that for the pre-MODIS era, CLARA-A2 has additional observations available from NOAA-12 and NOAA-15 relative to Pathfinder (and additionally NOAA-17, NOAA-19 and METOP-A & B for the MODIS era).

The issue of correctly detecting clouds over bright snow/ice is a consideration for any AVHRR-based study; while some concerns remain on cloud detection accuracy over the high-elevation regions of Greenland (Karlsson et al, 2017), neither the in situ evaluations nor the stability evaluation undertaken here suggest that the large-scale CLARA-A2 ice sheet albedo estimates are significantly influenced by missed clouds. This is likely linked to the leveraging of all AVHRR satellites and the coarsened end product resolution, where typically hundreds or even thousands of reported clear-sky AVHRR GAC-resolution samples are aggregated in a 25 km resolution grid cell to form the grid cell monthly mean albedo. While missed clouds will certainly appear in the data, their impact at the end product scale is ameliorated by the majority of correct clear-sky samples. The 5-day means are more vulnerable to this effect, though, which is partially why statistical Gaussian Process smoothing was applied to the 5-day data in the manuscript.

The spatiotemporal consistency of albedo trends between CLARA and MOD10A1 also reinforces the idea that cloud masking issues are not a dominant driver of the observed trends.

9 19-26 bringing in Stroeve2001 agreement/disagreement seems important here Stroeve found NAO resonance,as one would expect. What about this study?

Please see the remarks above. To make these points to the reader as well, we will include a new paragraph here (pg 10, 7-16) summarizing these differences/likely causes relative to Stroeve (2001).

Also, note that some remarks on the cloud masking are also included in the discussion section for clarity.

C.) conclusions . . . 16 12 “The albedo decrease of the northeastern and eastern mar-gins was initiated during the 1982-1999 period” . . . you offer a mechanism for the west but what about the east...any idea the cause? It should be either/and atmospheric circulation or sea ice -related.

This is a very good question, to which we presently have no clear answer. The topography of the SE/E coast is quite complex, and while CLARA-A2 SAL does contain a correction algorithm for both geolocation and radiative impacts of mountainous topography (areas with mean slope>5 deg), we remain bound by the overall geolocation accuracy of AVHRR. This implies that we cannot discount sampling errors as a source of influence in complex terrain.

Yet there is some similarity in the negative albedo trends around Blosseville coast in MOD10A1 and CLARA (see next point), some of which are also reproduced by the earlier studies noted here based on various versions of the Pathfinder dataset – although the comparability is limited, as noted in the previous point.

On the other hand, Häkkinen and Rhines (2009) showed that the warm subtropical (surface) waters have begun to penetrate the seas around SE Greenland with increasing intensity, and Straneo et al. (2010) found them present in the Helheim glacier fjord. We could therefore postulate that when the increasing heat energy thus advected on the SE coast is released into the atmosphere, it provides additional energy for the surface melt of snow. This would be consistent with the localized but substantially negative albedo trends seen around Helheim and Kangerdlussuaq glaciers in both MOD10A1 and CLARA-A2. Note that the increasing precip only affects the coast south of Helheim glacier according to MERRA-2.

The case of the NE margins appears different in that oceanic forcing is less likely a cause; we noted that some modeling studies found increasing runoff and thus surface melt, and if downslope winds were increasing along with positive air temperatures, the turbulent flux exchange could also accelerate melt. In this perspective, MERRA-2 does show a statistically significant if unremarkable positive trend in SAT over the NE region (here shown for 78-79.5N, -29 to -32 E, July & August). However, the veracity of the wind fields is untested and thus the quantification of turbulent flux contribution is an uncertain process.

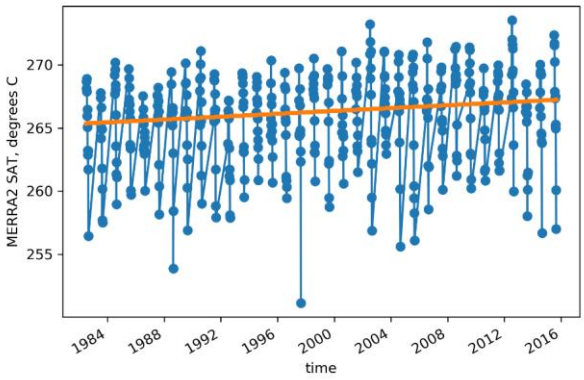

We propose to add new content in the results section (3.1, pg.9) and the discussion section (pg 16) summarizing the arguments here.

D.) A direct comparison between albedo data sets: CLARA-A2-SAL and MODIS MOD10A1 seems warranted. How well do they agree in the overlapping period?

We performed a comparison between the datasets, showing the results here for the reviewer's interest, and also propose to add them as supplementary material in the manuscript (Supplementary Figure 4), with commentary in the discussion section (pg 16, 9-17). This is motivated by the fact that a rigorous intercomparison should account for factors which require substantial additional work to quantify, e.g. differences in diurnal sampling, and analysis for the impacts of various downscaling methods to reduce MOD10A1 into the coarse CLARA grid.

We calculated the decadal Theil-Sen albedo trend estimators for the 2000-2015 May-August months for MOD10A1 in its native 5km resolution on the polar stereographic grid (Box et al., 2017, denoised, gap-filled). For the calculation of per-month mean differences during the 2000-2015 overlap, we resampled MOD10A1 to the CLARA grid with a radial weight algorithm with a 25 km radius. While this choice should be broadly acceptable, we note that a more careful intercomparison is deserving of a separate manuscript.

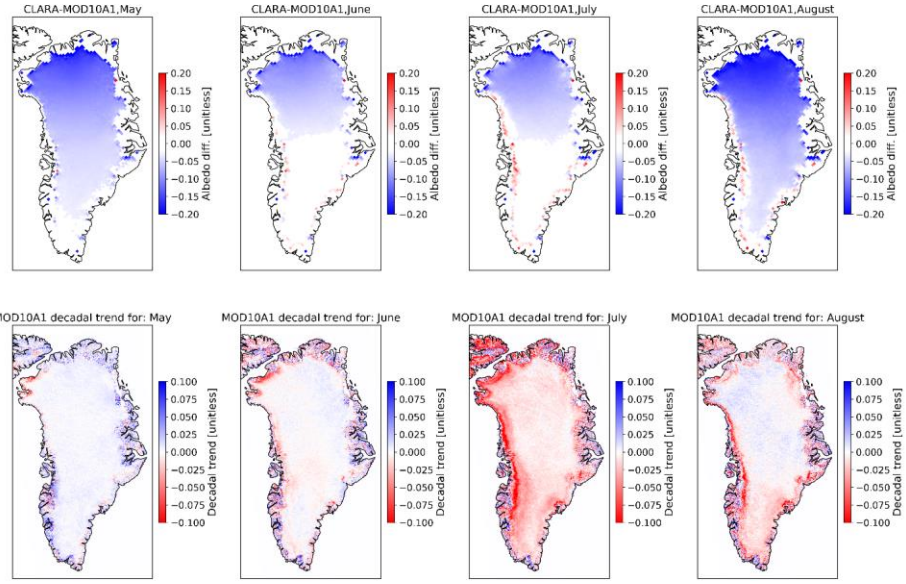

The spatiotemporal distribution of the decadal trends is highly similar. Most of the small-scale albedo decrease features, such as decreases around Helheim and Kangerdlussuaq glaciers, are consistent if limited by the coarse CLARA resolution. The trends in MOD10A1 have larger maxima than CLARA-A2 most likely because of the considerably finer spatial resolution (5 km vs. 25 km) – in CLARA-A2, the narrow regions of sharpest albedo decreases at the (west) margins are smoothed by the spatial aggregation.

The by-month mean difference maps (top row) only show differences above an estimated joint CLARA/MOD10A1 uncertainty envelope of 0.03. As expected considering the results by Alexander et al. (2014), the difference is large in the North during May and August. This difference is stable, though, and does not appear to impact the decadal trends, which agree even for the large-difference regions.

General comments

7 16 agree with "empirically suitable threshold albedo of 0.58" . . . compositing with many PROMICE years yields 0.56 (unpublished)

Thank you, this information is good to know also for future reference.

Recommend to not use abbreviation "GrIS". Instead, use "Greenland ice sheet" until it (very quickly) becomes obvious the study is on Greenland, afterw ard, use "ice sheet". Should title have"mass balance" io "surface mass balance and ice discharge"

GrIS -> Greenland Ice Sheet revised as suggested throughout the manuscript. How ever, the title is in our view accurate; the proxy investigation is limited to surface mass balance only, and the manuscript contains a comparative investigation of annual ice discharge and albedo anomalies, even though the time-lag analysis has been removed according to the review er's critique.

1 9 "driven in part by " io "primarily driven by "

Revised as suggested.

1 13 "We then subtract ice discharge from the mass change estimates from the GRACE satellite mission to estimate surface mass balance" io "We then correct the mass balance estimates observed by the GRACE satellite mission w ith state-of-the-art ice discharge"

Revised as suggested.

1 23 "rapid surface mass" io "rapid mass"

Revised as suggested.

2 31 "examining the role of albedo" io "both highlighting and confirming the dominant role of surface melt" w ould seem to improve the statement by making it not a conclusion placed in the intro of the paper and otherw ise clarifying that albedo is the predictor variable here.

Revised as suggested, proposing to amend "albedo" to "albedo-inferred", as albedo is a proxy for surface runoff here.

4 1 "uppermost areas" io "innermost parts"

Revised as suggested.

4 1 - 4 8. . . Fig3A in Box, J.E., D. van As, K. Steffen, 2017. Greenland, Canadian and Icelandicland ice albedo grids (2000-2016), Geological Survey of Denmark and Greenland Bul-letin, 38, 53-56 available from http://w ww.geus.dk/DK/publications/geol-survey-dk-gl-bull/38/Documents/nr38_p53-56.pdf supports the idea that 2012 w as not anomalously low AND that variability is small (in the Summit GC-Net example; max-min = 0.03) in the dry snow area'

Thank you for the additional reference, added to the text here.

4 12 “~0.02 increase of the GrIS albedo” io “~0.02 overestimation of the GrIS albedo”. . . it was a real climate event so the measurement is not an over-estimation

While the reasoning by Stroeve (2001) that the Pinatubo eruption caused cooling which inhibited e.g. Greenland melt for 92-93 is principally valid, the relatively large albedo increase on the top of the accumulation zone in CLARA-A2 for these years (Fig 1) is difficult to fully explain in terms of less surface melt or snow metamorphism– as we normally expect negligible surface melt or metamorphism there anyway. The Pathfinder as well as CLARA records are based on climatological mean aerosol loading over the Arctic – for want of a reliable and spatiotemporally complete aerosol record reaching the 80s – so that some part of the albedo increase could also be explained by unaccounted-for change in atmospheric composition. As the albedo estimates for these years are thus more uncertain than the rest of the CLARA record, we prefer keeping the analysis and text here as is, with some additional explanation for the logic w.r.t. the discussion here (pg 4, 11-21).

8 25 I expect some readers/reviewers will dislike excluding 92 and 93. Yet,I think it’s not too questionable as long as you’re clear. Here, better I think would be“externally forced” io “less reliable”

Please see the point above. We propose amending the mentioned text to “likely both externally forced and less reliable” to account for both possible explanations.

8 25 “largely remained stable” discuss relative toStroeve 2001

Revised w.r.t. the discussion around major comment B.

8 31 “may be”? Seems more testing needed to address this hypothesis.

Revised w.r.t. the discussion around major comment D, relocated to the discussion section.

9 1 “is” io “may be”. . . see/cite Box, J.E., D. van As, K. Steffen, 2017. Greenland, Cana-dian and Icelandic land ice albedo grids (2000-2016), Geological Survey of Denmarkand Greenland Bulletin, 38, 53-56

Relocated to discussion section.

9 5 “rarely examined” “the ice sheet’s albedo was primarily stable” see Fig 9c and related discussion in the following where from 1988-1999 eastern Greenland has the largest AVHRR albedo decrease. Some discussion of that seems warranted. Box, J.E., D.H. Bromwich, B.A. Veenhuis, L-S Bai, J.C. Stroeve,J.C. Rogers, K. Steffen, T. Haran, S-H Wang, 2006: Greenland ice sheet surface massbalance variability (1988-2004) from calibrated Polar MM5 output, Journal of Climate,Vol. 19(12), 2783–2800.

Thank you, the authors did not recall that the stated study also contained satellite-based data evaluation. We note that the limitations on Pathfinder/CLARA comparisons as discussed in response

response to major comment B also likely apply here. However, this reference will naturally be added here and the manuscript revised to reflect these past efforts. The sentence "primarily stable" will be revised to enhance that the finding is only based on CLARA data, and that significant negative albedo trends are apparent on the NE and E margins – in itself the E decreases being consistent with the Pathfinder analysis in the given manuscript.

9 28-34 geolocation errors were attributed in the following study for the relatively noisy ice margin trends. See Box, J.E., D.H. Bromwich, B.A.Veenhuis, L-S Bai, J.C. Stroeve, J.C. Rogers, K. Steffen, T. Haran, S-H Wang, 2006:Greenland ice sheet surface mass balance variability (1988-2004) from calibrated PolarMM5 output, Journal of Climate, Vol. 19(12), 2783–2800.

Certainly they may contribute; the referenced discussion will also be noted as a potential cause of the effect seen. The discussion section now contains the reference as a part of a new paragraph summarizing the MOD10A1-CLARA comparison (pg 16).

10 7 "where the trend signal originates" io "where they are expected to be more robust"

Revised as suggested.

10 10 "larger" io "faster"

Section revised for clarity, phrase removed.

10 21 "earlier" io "faster"

Faster is our preferred term; Figure 7 clearly shows increases in albedo decrease rate (per 30 day period).

10 25 the "increases in winter snow fall" finding is very interest-ing AND is related to the GRACE correlation because when there is snow fall, mass is added and albedo increases. So, be sure to make that point. The following may be relevant if you want to discuss more about how increasing snow fall may be from climate change. https://iopscience.iop.org/article/10.1088/1748-9326/10/11/114008/meta Fur-ther Box et al. (2013) find a climate change signal, an increase in snow fall with NH AirT, N Atlantic Air T, etc. Comparison of Greenland accumulation history with northernhemisphere air temperatures suggests a 6.8% (or 51 Gt) per degree C climate sen-sitivity (Box et al., 2013). See Box, J. E. 2013. Greenland ice sheet mass balancereconstruction. Part II: Surface mass balance (1840-2010), Journal of Climate,Vol.26, No. 18. 6974-6989. doi:10.1175/JCLI-D-12-00518.1

Thank you, the reference has been added. The work by Wong et al. has been referenced in a new paragraph in the discussion section (pg 13, 16-22) on the NW bare ice exposure changes in context of observed precip trends – which appear quite different from MERRA-2 over the region.

15 20-26 Including discus-sion of Rajew icz and Marshall, 2014; McLeod and Mote 2016 is w arranted. e annual frequency of extreme high pressure 'blocking event' days that deliver w arm air onto w estern Greenland peaked in 2010 and 2012 (McLeod and Mote, 2016). Greenland mass loss accelerated betw een 2003 and 2012 primarily due to increasing surface meltw ater runoff (-6.3±1.1 Gt/y2) driven by persistent southerly flow across the w estern ice sheet (e.g. Rajew icz and Marshall, 2014; McLeod and Mote, 2016). McLeod,J.T. and T.L. Mote, 2016. Linking interannual variability in extreme Greenland blocking episodes to the recent increase in summer melting across the Greenland ice sheet.International Journal of Climatology, 36:1484-1499. Rajew icz, J. and S.J. Marshall,2014. Variability and trends in anticyclonic circulation over the Greenland ice sheet,1948–2013. Geophysical Research Letters, 41:2842-2850.

Thank you, the additional references are added and the raised points noted in the revised manuscript (discussion section, pg 15, 27-34)).

16 20 "A notable exception to the w idespread albedo decrease w as" io "A notableexception w as"

Revised as suggested.

Figures Fig 2, 4,6 Increase text size.

Revised as suggested.

In Fig 4 a tiny a, b, c . . . text is problematic.

Text size increased.

Figs3-5 w ould be an improvement to zoom in to the island of Greenland in each map

Revised the figures to provide a tighter zoom on Greenland itself.

Fig 4 inset trend map too small? The analysis is v interesting and deserves highlight. Maybe too many maps compressing the results too much. Remove the grey area.

Thank you. The Figure w as split into independent figures per period, also providing the inset figure as an independent figure.

Fig 5 units per day? Small number, multiply to get per month?

Revised to reflect change per 30-day period.

Fig 7 sorry but I think this analysis does not add sufficiently to the study

In line with the earlier comment and feedback from Reviewer 1, we have omitted this analysis and the corresponding figures from the manuscript.

List of relevant changes in manuscript:

1. Removed time-lag analysis of seasonal basin-scale ice discharge and surface albedo anomalies, as requested by reviewers and editor.
2. Comprehensively revised text on proxy SMB analysis. Text now stresses the intended use as an observation-driven test on the role of surface melt in summer SMB variability, includes cautionary remarks on the limits and applicability of the method, and expands on the treatment of other connections between SMB terms and albedo, as requested by reviewer Box. Regression equations relegated to supplementary material. (Section 1, 2.7.4, 3.3. & 4)
3. Expanded discussion of results relative to previous works in the field, e.g. Stroeve (2001), Straneo et al. (2011), Rajewicz and Marshall (2014), Wong et al. (2015), McLeod and Mote (2016), Box et al. (2006;2017) (Sections 3.1 and 4 mainly).

Other changes include typo corrections, clarifications of expressions and grammar corrections.

The surface albedo of the Greenland Ice Sheet between 1982 and 2015, and its relationship to the ice sheet's surface mass balance and ice discharge

Aku Riihelä[1], Michalea D. King[2], Kati Anttila[1]

[1]Finnish Meteorological Institute, Helsinki, FI-00560, Finland
[2]Byrd Polar and Climate Research Center, Columbus, USA.

Correspondence to: Aku Riihelä (aku.riihela@fmi.fi)

Abstract. The Greenland Ice Sheet is losing mass at a significant rate, ~~primarily driven by~~driven in part by increasing surface melt-induced runoff. Because the ice sheet's surface melt is closely connected to changes in the surface albedo, studying multidecadal changes in the ice sheet's albedo offers insight into surface melt and associated changes in its surface mass balance. Here, we first analyse the CLARA-A2 SAL satellite-based surface albedo dataset, covering 1982-2015, to obtain decadal albedo trends for each summer month. We also examine the rates of albedo change during the early summer, supported with atmospheric reanalysis data from MERRA-2, to discern changes in the intensity of early summer melt, and their likely drivers. We find that rates of albedo decrease during summer melt have accelerated during the 2000s relative to early 1980s, and that the surface albedos now often decrease to values typical of bare ice at elevations 50 – 100 m higher on the ice sheet. The southern margins exhibit the opposite behaviour, though, and we suggest this is due to increasing snowfall over the area. We then ~~correct~~ subtract ice discharge from the ~~the~~ mass balance estimates observed by the GRACE satellite mission ~~with state-of-the-art ice discharge estimates to obtain observation-based estimates for the~~to estimate surface mass balance. The CLARA albedo changes are regressed with this data to obtain a proxy surface mass balance timeseries for the summer periods 1982-2015. This proxy timeseries is compared with latest regional climate model estimates from the MAR model to perform an observation-based test on the dominance of surface runoff in the magnitude and variability of the summer surface mass balance. ~~We show that t~~The proxy timeseries agrees with MAR through the analyzed period within the associated uncertainties of the data and methods, ~~demonstrating and~~ confirming that surface runoff has dominated the rapid surface mass loss period between 1990s and 2010s.

Finally, we extend the analysis to the ~~GrIS~~ drainage basin scale to examine discharge-albedo relationships in order to ascertain if the surface melt contributes to discharge acceleration via basal lubrication. ~~While there is~~ We find little evidence of surface melt-induced ice flow acceleration at annual timescales~~, we find time lags between seasonal maximum runoff production and seasonal maximum discharge rate to be in agreement with recent modelling results.~~

1. Introduction

The surface albedo of the Greenland Ice Sheet's ablation area has been shown to play a crucial role in determining melt variability through the snow/ice albedo feedback effect (Box et al., 2012). The study of these albedo changes over the last decade and a half from modern satellite sensors such as MODIS has drawn considerable research attention (Box et al., 2006; Tedesco et al., 2011; Stroeve et al., 2013; Alexander et al, 2014; Tedstone et al., 2017, Casey et al., 2017). The observed albedo decreases are closely tied to the increasing mass loss of the ice sheet through the enhancement of its surface melt (Enderlin et al., 2014; van den Broeke et al., 2016). The ice sheet also loses mass through the ice calving at outlet glaciers, or discharge, the magnitude of which has recently been shown to demonstrate significant spatial and seasonal variability (King et al., 2018). The mass loss of the Greenland Ice Sheet ~~(henceforth GrIS)~~ has been shown to currently be among the leading contributors to sea level rise (Box et al., 2017).

Legacy satellite sensors such as AHVRR offers us the possibility to study the ~~GrIS~~ Greenland ice sheet's albedo changes of over a period of more than three decades, doubling the temporal coverage of MODIS. The drawback is lower spectral precision and coverage. Yet, considerable efforts have recently been paid to the intercalibration of the AVHRR sensor family (Heidinger et al., 2010), greatly improving the sensors' capabilities to detect long-term trends in surface albedo. Here, we use the sensor-intercalibrated 34-year (1982-2015) surface albedo data record from the CLARA-A2 dataset family (Karlsson et al., 2017) to study the albedo changes of the ice sheet at decadal scales.

Formatted: Font: Not Bold

Our analyses focus on the summer months between May and August (MJJA), comprising four topics. First, we calculate and present the trends in surface albedo (defined here as the directional-hemispherical reflectance of the surface, i.e. black-sky albedo or 'inherent' albedo) over the ~~GrIS~~ ice sheet for each respective month. In addition to the trends for the full 1982-2015 period, we present temporally subsetted trends consistent with the MODIS observation era (2000-2015) and the pre-MODIS era (1982-1999), in part to compare our results with the trends identified from the latest editions of MODIS data (Casey et al., 2017) and also to offer a rare, if somewhat more uncertain, look into the ice sheet's surface changes in the 80s and 90s. Treating each month individually additionally allows us to delineate between albedo changes in the early and late melting season.

Second, we examine changes in melt intensity and speed through changes in the rate of albedo decrease and in the spatial distribution of albedo values indicative of bare ice and wet snow as the summer melt progresses. At this stage we also analyse atmospheric reanalysis data to discern if the observed changes may be explained by precipitation or air temperature anomalies.

Third, we conduct an observation-driven test for the dominance of surface runoff in the interannual variability of May-August surface mass balance (SMB) of the ice sheet. We calibrate discharge-corrected, gravimetrically observed SMB with the CLARA surface albedo to form a summer-aggregated proxy SMB. When compared against the SMB from a state-of-the-art

regional climate model for the ice sheet (MAR, Fettweis et al., 2017), we expect to find good covariability only if surface runoff dominates SMB variability, as that is the sole term which can be considered well-correlated with albedo changes. ~~show that, when calibrated against discharge-corrected state-of-the-art gravimetric observations of the ice sheet, the CLARA surface albedo estimates can serve as a useful stationary proxy for the summer surface mass balance (SMB) changes during its 34-yr coverage. The SMB estimates achieve good agreement with the MAR regional climate model (Fettweis et al., 2017) for the study period, both highlighting and confirming the dominant role of surface melt in the recent acceleration of the GrIS summer mass loss.~~

Finally, we downscale the analysis to six major drainage basins of the ice sheet. ~~Having demonstrated~~Again assuming that surface albedo changes are an acceptable proxy for surface runoff production, we examine the albedo-discharge relationships to ascertain from observational basis if inferred surface melt anomalies correlate ~~to seasonal maximum ice export~~with the interannual variability in ice discharge.

2. Data and Methods

2.1. CLARA-A2 SAL surface albedo dataset

The satellite-based surface albedo data used here is the Satellite Application Facility on Climate Monitoring (CM SAF) cLoud, Albedo and surface RAdiation data record CLARA-A2 SAL, funded by the European Organization for the Exploitation of Meteorological Satellites EUMETSAT. It covers the years 1982-2015 and is based on intercalibrated AVHRR data. The retrieved albedo is defined as directional-hemispherical albedo for the wavelength range 0.25 -2.5 µm (for snow and ice), and the observations are provided in a 0.25° latitude-longitude or a 25 km EASE-~~2~~ grid for the Polar Regions. The algorithm accounts for topography corrections over mountainous regions as well as dynamic aerosol depth (Jääskeläinen et al., 2017). However, over the Arctic where dynamic aerosol loading is difficult to estimate and typically exhibits a limited variability, a constant value of 0.1 at 550 nm is used.

The albedo of snow- and ice-covered areas is derived by averaging the broadband bidirectional reflectance values of the AVHRR overpasses into 5-day or monthly means, relying on wide AVHRR swaths and temporal aggregation to provide dense sampling of the viewing hemisphere~~.~~. The dense sampling is combined with a narrow-to-broadband conversion algorithm which ~~forms~~adapts for wet and dry snow/ice surfaces (Xiong et al., 2002) to form~~, which forms~~ the albedo estimate (Riihelä et al., 2013). The sampling rate has been further improved by the expansion of the AVHRR constellation from the mid-1990s onward. The CLARA dataset uses data from NOAA-7 to NOAA-19, as well as METOP A and B (Karlsson et al., 2017). A critical feature of the CLARA dataset family is that it is based on an intercalibrated Fundamental Climate Data Record (FCDR) of observed AVHRR radiances, where the calibration differences between satellites have been removed by use of a variety of techniques (Heidinger et al., 2010).

The data record has been validated against in situ data (Anttila et al., 2016) and compared to the MODIS black sky albedo product MCD43 (Schaaf et al., 2002). Comparisons between CLARA-A2 SAL and in situ measurements on ~~GrIS~~ the ice sheet have yielded RMSE between 0.04 and 0.07 over the more stable accumulation zone with no obvious systematic over- or underestimation tendencies, and a RMSE of ~0.11 over a site (JAR2) in the ablation zone. It should be noted that it has recently been shown that point-to-pixel evaluation of surface albedo retrievals over the heterogeneous surfaces of ~~GrIS~~ the ablation zone, particularly in the southwest, cannot be expected to yield true estimates of retrieval quality when the spatial resolution of the estimate is in the kilometre range (Moustafa et al., 2017), as is certainly the case for CLARA-A2 SAL.

A critical attribute for the surface albedo timeseries from the viewpoint of trend determination is its stability. Here, we demonstrate the stability of CLARA-A2 SAL by examining the monthly mean albedo over a small region in the central part of ~~GrIS~~ the ice sheet between 73 and 75 degrees North latitude, and 38 and 42 degrees West longitude. The ~~innermost~~ ice sheet's uppermost parts ~~of GrIS~~ have a naturally stable surface albedo, and therefore variations in the albedo estimates may be considered to primarily result from algorithm uncertainty. The mean surface albedo for this area is shown as a timeseries in Figure 1 for the months between May and August (MJJA). As can be seen, the variability about the 34-yr interannual mean largely falls within the reported 5% (relative) accuracy, although individual grid cell-scale albedo retrievals may display larger uncertainty as a function of cloud masking efficiency, surface sampling rate, and uncertainty in the atmospheric correction of the satellite imagery. Still, we observe no obvious trends in the albedo of this region. The widespread surface melt of 2012 was relatively short-lived over this area (Bennartz et al., 2013), and thus did not appreciably impact the albedo, as also shown from MODIS data (Box et al, 2017).

A notable deviation from the interannual mean albedo occurs over the years 1992 and 1993. The cause of this is known. The eruption of Mt. Pinatubo, on June 15, 1991, injected vast quantities of aerosols and dust into the atmosphere. This altered the atmospheric composition on a global scale for the next 2-3 years. Stroeve (2001) attributed a concurrent increase in observed Greeland Ice Sheet albedo to the cooling effect of the additional stratospheric aerosols. While we see a similar effect in the CLARA data, it should be noted that the atmospheric correction necessary to derive surface reflectances from AVHRR observations in CLARA depends on the aerosol loading being correct. Larger aerosol loading conditions over bright snow are challenging for the atmospheric correction algorithms. ~~, and is manifested here as a ~0.02 overestimation of the GrIS albedo during these years. Therefore,~~ It is difficult to deconvolve cooling-induced albedo increase from potential artifacts resulting from an incomplete characterization of the atmosphere. ~~w~~We ~~henceforth~~ therefore exclude these years from the analysis but otherwise conclude that the time series appears stable enough for trend analysis. The observed variability envelope shall form the first, but not only, boundary condition for evaluating the significance for any obtained trends, as explained in detail in section 2.7.2.

To exclude the non-glaciated surfaces of Greenland from the analysis, the PROMICE ice mask (Citterio and Ahlstrøm, 2013) was resampled into the CLARA grid and all grid cells with a fractional ice cover of less than 50% were discarded. We also attached surface elevation data into the CLARA dataset from CLARA grid-resampled DEM by Helm et al. (2014).

2.2. MAR regional climate model

The regional climate model data comes from the Modèle Atmosphérique Régional (MAR) model (version 3.5.2) (Fettweis et al., 2017). Here, we use the model run data forced with the ERA-Interim atmospheric reanalysis for the period 1979-2014. To obtain the MJJA surface mass balance from MAR, we first extract the monthly surface mass balance fields, correct for the variation in grid cell areas in the model domain, mask out all grid cells with fractional ice cover less than 50% for consistency with the CLARA data, and sum the MJJA output.

2.3. ~~GrIS i~~Ice discharge estimates

Here we use continuous estimates of ice discharge from all large Greenland outlet glaciers over the 2000-2015 period, taken from King et al. (2018). These glacier-scale time series are derived by incorporating changes in glacier velocity, from both radar and optical imagery, and changes in glacier thickness calculated from time-varying surface elevation data. With high temporal and spatial resolution, these records allow for ~~GrIS~~ice sheet-wide and basin-scale sub-monthly changes in ice discharge, hereafter referred to as D, to be compared with albedo-based meltwater proxies.

2.4. MERRA-2 atmospheric reanalysis and the Greenland Blocking Index (GBI)

The Modern-Era Retrospective analysis for Research and Applications, Version 2 (MERRA-2) is a global atmospheric reanalysis of the modern satellite era, covering the period from 1980 to present day (Gelaro et al., 2017). Operating at 72 atmospheric levels with a spatial resolution of 0.5 by 0.625 degrees, MERRA-2 ingests a wide variety of satellite observations and features e.g. observation-based corrections of the model precipitation field and a sophisticated treatment for atmospheric aerosols.

The representation of glaciated surfaces has also received substantial attention in the development of MERRA-2 (Cullather et al., 2014). It was also recently shown that the surface air temperatures (SAT) in MERRA-2 are well aligned with station observations across the ~~GrIS~~ ice sheet (Reeves Eyre and Zeng, 2017). For these reasons, we selected MERRA-2 to provide (winter) precipitation and SAT data for our analysis.

The Greenland Blocking Index (GBI) used here is defined as the weighted mean 500 hPa geopotential height over a region bounded by 60 – 80 °N and 20 – 80 °W. The dataset is obtained from NOAA Earth System Research Laboratory (ESRL) and based on Hanna et al. (2013).

2.5. ~~GrIS m~~Mass balance estimates from GRACE satellite observations

The gravimetric mass balance data used here are from the Greenland Ice Sheet Climate Change Initiative (CCI) project, based on Gravity Recovery and Climate Experiment (GRACE) satellite pair measurements and the GRACE ITSG-Grace2016 gravity field model (Mayer-Gürr et al., 2016). The data covers 2003-2015, as prepared by the Technical University of Dresden (Groh and Horwath, 2016).

The CCI mass balance estimates are based on a point mass inversion method after Forsberg and Reeh (2007), Sørensen and Forsberg (2010), and Barletta et al. (2013). A notable feature in the use of GRACE for ~~GrIS~~ the mass loss estimation is that the gravimetric signals from outer ice caps and small glaciers are not distinguishable from the ice sheet gravity changes. However, on the scale of the whole ice sheet, the optimal mass balance solution needs to contain this contribution. As the ~~GrIS~~ ice sheet extent defined for CLARA also contains any outer glacier or ice cap grid cells if their ice coverage is sufficiently large, there is no major discrepancy in the combined use of GRACE and CLARA data.

2.6. ~~GrIS s~~Surface albedo dataset from MODIS (MOD10A1)

We obtained the latest (Collection 6) MODIS-based ~~GrIS~~ ice sheet surface albedo data from the MOD10A1 timeseries (Hall et al., 1995) ~~in order to repeat the analysis by Colgan et al. (2014) and compared these results to~~ for comparison the CLARA-A2 SAL. ~~SAL-based GrIS surface mass balance proxy.~~ These data are provided in 5 km spatial resolution as daily means between 2000 and 2017, and feature denoising, gap filling and bias correction procedures as described in Box et al. (2017). For ~~consistency~~ the comparison, these data are ~~also~~ reprojected to the 25 km CLARA grid with radial weight resampling and grid cells with ice cover less than 50% were discarded.

2.7. Methods

2.7.1. Study area definitions

As mentioned, here we define ~~GrIS~~ the ice sheet extent through the use of the PROMICE ice mask (Citterio and Ahlstrøm, 2013) using a threshold of 50% for fractional ice cover as the inclusion condition. Basin-scale analyses were done using the six basin boundaries based on Sasgen et al. (2012), with the modification that we combine their basins D and E into our basin 4. The basin delineation and ~~GrIS~~ ice sheet extent are illustrated in Figure 2.

2.7.2. Trend assessment

All trends shown here have been calculated as Theil-Sen estimators, i.e. as the median of all possible slopes between data pairs in the examined dataset (Theil, 1950; Sen, 1968). The Theil-Sen estimator is robust against outlier influence compared to ordinary least squares regression. This feature is highly useful in trend analysis of CLARA-A2 SAL data over the ice sheet, where misclassified clouds may contribute ~~.~~ noise into the clear-sky surface albedo estimates (Karlsson et al., 2017).

The trends in surface albedo were deemed significant only if both of the following conditions were met. First, the observed trend slopes were non-zero at the 95% confidence interval. Second, the decadal albedo trends were larger than 0.015 per decade. The latter condition largely follows the analysis by Casey et al. (2017) for the MODIS Collection 6 ~~GrIS~~ surface albedo, who considered a decadal trend of 0.01 as the limit of MODIS observability. We have tightened that limit to 0.015 for CLARA to account for the less precise radiometric accuracy of AVHRR, which remains even after the considerable intercalibration work done on the CLARA input radiances (Heidinger et al., 2010). We finally note that while the observed trend magnitudes were largely insensitive to the choice of CLARA input data (5-day or monthly means), monthly means are used for the decadal trend calculations when shown here.

2.7.3. Melt rate and ice exposure calculations

In order to examine changes in the intensity of melt across the ~~GrIS~~ ice sheet margins during our 1982-2015 study period, it is necessary to estimate two parameters: the melt rate, expressed as albedo decrease per day during the melting season, and a yes/no condition for determining if a particular area of ~~GrIS~~ the ice sheet melted substantially enough to be composed primarily of bare ice and wet snow. The detection of melt onset ~~over GrIS~~ is challenging, as reductions in albedo typically begin gradually and sporadic snowfall events may 'reset' the albedo to the pre-melt range. We tested the use of a sophisticated Gaussian Process (GP)-based change point detection algorithm implemented after Fearnhead (2006) and Xuan and Murphy (2007), but the gradual impact of melt onset in the albedo data proved too difficult to capture with such a probability-based change point detection method.

We then implemented a simpler scheme, in which the 5-day albedo record between May-August for each grid cell and year is first smoothed with a GP regressor algorithm with a Mátern kernel to contain 120 data points, corresponding to a temporal resolution of ~1 day. The smoothed data series is evaluated to find the first sample after early May for which the albedo value deviates more than two standard deviations from the preceding early-summer albedo mean. The melt rate estimate is then taken to be the albedo difference between that value and the summer minimum albedo, divided by the time between the two events. As this method may be expected to provide reasonable melt rate estimates only for the ice sheet margins where significant seasonal albedo dynamic exists, we present the melt rates only for areas where the surface elevation is less than 2200 m a.s.l.

~~This smoothed timeseries was also applied to the basin-scale examination of the relationship between ice discharge rate and albedo changes. Specifically, we estimated the timing of fastest albedo decrease as a proxy for maximum runoff production by finding the day (limited between May and mid-August) in the smoothed, basin-averaged albedo data on which the albedo decrease rate first reached 95% of its annual maximum. To enhance the albedo dynamic, grid cells with elevations larger than 2800 m were excluded from the aggregation.~~

For the detection of bare ice and wet snow surfaces, we first note that melting bare ice surfaces around the ~~GrIS~~ ice sheet margins generally have surface albedos in the range of 0.5 to 0.65 (Bøggild et al., 2010), although significant amounts of impurities at the ice surface may of course further reduce the albedo. This albedo range is also applicable for wet snow areas with significant melt ponding. We therefore selected an empirically suitable threshold albedo of 0.58 and observed the CLARA grid cells in which the surface albedo reaches this value for each year in the study period. Changes in the melt rate and distribution of bare ice/wet snow areas were studied by comparing three-year means at the beginning and end of the full study period (1982-2015), as well as the MODIS (2000-2015) and pre-MODIS (1982-1999) eras. For the continuous melt rate estimates, trends for these time periods were further determined using the Theil-Sen estimator as described in section 2.7.2.

2.7.4. Forming a surface mass balance proxy from surface albedo observations to test surface runoff dominance in summer-aggregated SMB

The mass balance of ~~GrIS~~ the ice sheet may be expressed as (e.g. van den Broeke et al., 2017)

$$MB = \frac{dM}{dt} = SMB - D \quad (1)$$

Where SMB is the ice sheet's surface mass balance, and D represents the summed solid ice discharge from all large marine-terminating outlet glaciers. Furthermore, the surface mass balance may be expressed as (e.g. van den Broeke et al., 2017)

$$SMB = P_{tot} - SU_{tot} - ER_{ds} - RU \quad (2)$$

Where P_{tot} is the sum total of snowfall and rainfall, SU_{tot} represents the total sublimation, ER_{ds} represents surface snow mass lost via wind-driven erosion, and RU represents meltwater runoff.

An earlier study by Colgan et al. (2014) presented the idea that, because of the very strong impact of surface melt on the ice sheet's surface mass balance (e.g. van den Broeke et al., 2016), the ice sheet average surface albedo could serve as a meaningful and stationary proxy for the melt season mass balance (MB) dynamic when calibrated against gravimetric mass balance observations from the Gravity Recovery and Climate Experiment (GRACE) satellite pair. However, the full mass balance of the ice sheet includes dynamic ice losses from glacier discharge, to which surface albedo is insensitive. ~~We therefore propose to e~~Expanding on the original idea, ~~by directly~~ we correlated~~ing~~ CLARA-observed surface albedo and GRACE-based SMB changes in order to infer a proxy SMB time series from the CLARA surface albedo dataset, for the purpose of testing if surface melt variability is the dominant term in (summer) SMB variability. ~~, covering its full 34-year duration and thus reaching further back in time than either GRACE or a MODIS-based proxy. The method is limited in scope to the summer months (May-August), and is predicated on the dominant influence of runoff in SMB variability during the satellite era (Box, 2013).~~

To obtain the proxy, we first ~~correct~~ add the monthly ~~GrIS~~ MB change record from GRACE data ~~with~~ and he state-of-the-art discharge (D) estimates from recent work by King et al. (2018) to obtain a GRACE-based SMB estimate. Then, a linear regression is sought between the new GRACE SMB estimate and CLARA monthly mean ~~GrIS~~ ice sheet albedo for all ~~summer~~

Formatted: Font: 12 pt
Formatted: Font: 12 pt
Formatted: Font: 12 pt
Formatted: Font: 12 pt
Formatted: Font: 12 pt
Formatted: Font: 12 pt
Formatted: Font: 12 pt
Formatted: Font: 12 pt
Formatted: Font: 12 pt
Formatted: Font: 12 pt
Formatted: Font: 12 pt
Formatted: Font: 12 pt
Formatted: Font: 12 pt

MJJA months in the overlap period 2003-2015 for which valid GRACE data exists (N=45). The regression period thus contains data from the period of rapid ~~GrIS~~ ice sheet mass loss in the 2000s, as well as from the years 2013-2015 when the mass loss had somewhat decelerated. The regression parameters are used to create summed MJJA surface mass balance proxy data from CLARA/GRACE for 1982-2015 for comparison with corresponding MAR SMB. The variability range observed for the central ~~GrIS~~ ice sheet albedo in CLARA (0.02) is taken to be the uncertainty range of the proxy SMB. For comparison, we also calculate and present the proxy SMB from the most recent MOD10A1 data as described earlier, using the same methods as for CLARA.

While surface albedo is correlated with surface runoff at the summer-aggregated scale, the relationship with the other SMB terms in eq. (2) is less certain. Albedo initially increases with snowfall, but saturates at fresh snow albedo levels (>0.8) once the fresh snow layer is optically semi-infinite, regardless of how much additional snowfall occurs after that. Rainfall produces the opposite effect, increasing mass but decreasing albedo, although at the summer-aggregated scale some of the rainfall near the ice sheet margins may be quickly lost as runoff, depending on the firn retention properties. The modelling-based finding that surface runoff dominates the MJJA surface mass loss (e.g. van den Broeke et al., 2017, and references therein) is therefore confirmed in this test only if the SMB proxy exhibits a strong degree of covariability with the MAR SMB.

It should be noted that use of this regression method is not suited for deriving a proxy SMB for a specific month or location on the ice sheet. This is particularly the case for the early summer (May), where surface melt is less important than precipitation for SMB changes. In terms of the MJJA aggregate, however, the early summer SMB variability is small compared to the total, thus incurring no greater uncertainty in the proxy than that already propagated from the albedo retrieval uncertainty itself.

~~We also calculate the proxy SMB from the most recent MOD10A1 data as described earlier. The obtained relationship is quite similar to that reported by Colgan et al. (2014) for MB, mainly because annual variations in GrIS discharge are relatively modest compared to the variability in SMB and albedo. The MODIS/GRACE proxy SMB is presented for comparison purposes for the period 2000-2017.~~

3. Results

3.1. Greenland surface albedo trends, 1982-2015

The Theil-Sen decadal albedo trend estimates are shown in Figure 3. Here, we omit the years 1992 and 1993 from analysis as their albedo estimates are likely both externally forced and less reliable. Over the full CLARA period, we note that ~~GrIS~~ ice sheet albedo has largely remained stable during the early summer months of May and June, though some of the outermost ice sheet margins in the North and East show statistically significant albedo decrease in June. However, in July and August, we

observe significant and negative albedo trends along most of the ~~GrIS~~ ice sheet margins. Analyzing the CLARA subperiods corresponding the pre-MODIS and MODIS eras (Figure 3, center and bottom rows), we find that the majority of the albedo decrease signal originates after 2000, with a strong albedo decrease (up to -0.05 / decade as an area average, individual grid cells may reach -0.1 / decade) along the Kangerlussuaq sector on the ~~GrIS~~ west margin. The MODIS era trends are consistent in magnitude and pattern with those presented by Casey et al. (2017) from the latest MOD10A1/MYD10A1 time series (see also supplementary material). ~~The negative trends in CLARA along the northern margin may be somewhat larger than those in MOD10A1. The cause may be in the tendency of MOD10A1 for retrieving relatively high albedo estimates for the northern parts of GrIS, a feature shown by Alexander et al. (2014) for the previous MODIS collection, which we note to remain valid for the current Collection-6 MOD10A1 for the month of August.~~

For the ~~rarely examined~~ pre-MODIS era of 1982-1999, we note that while the ice sheet's albedo was ~~primarily~~ mostly stable according to CLARA, significant~~ly~~ negative decadal trends in late-summer albedo (subplots (g, h) manifest over the Northeast ice sheet. The cause of this albedo decrease remains unclear at present. Based on in situ energy balance measurements over this area during summer of 1994, Konzelmann and Braithwaite (1995) argued that surface melt in the region was primarily driven by net radiative fluxes during a relatively cloudless summer, ~~but also that~~ They also note that the relatively high downslope wind speeds increase the importance of turbulent fluxes, possibly making the area more sensitive to near-surface air temperature anomalies. Mouginot et al. (2015) also reported an increase in modelled runoff in this area from the late 1980s onward, which is consistent with the negative albedo trend seen here. Some significant negative albedo trends are also apparent on the eastern margin, particularly along the Blosseville coast. Box et al. (2006) noted similar trends (in blue-sky albedo) based on an early version of the Polar Pathfinder extended (APP-x) dataset in the same area for the 1988-1999 period for the region. In contrast, though, they found no negative albedo trends in the Northeast.

Because the Theil-Sen trend estimator is defined as the median of all possible slopes between data points in a time series, the subperiod trends shown in Figure 3 do not necessarily sum up to the trends over the full 1982-2015 period. However, because the albedo trends from MODIS time series data have been extensively studied, we felt that presentation of the subperiod trends is important to compare results.

The subperiod division used here is also useful in that the clear change in late-summer albedo trends between 1982-1999 and 2000-2015 is fully consistent with a documented change in atmospheric regime over ~~GrIS~~ the ice sheet which began to favour high-pressure blocking patterns ~~over GrIS~~, as well as northward transport of warm and moist air, increasing near-surface air temperatures and enhancing downward longwave energy fluxes, all of which are features which promote surface melt (e.g. Box et al., 2012, Hanna et al. (2013), Mioduszewski et al. (2016), Välisuo et al. (2018)). Some of the other potential causes of the recent darkening of the western margin include increasing biological activity (algae growth; Ryan et al., 2018) and

previously deposited impurities emerging from the ice with each melting season, although recent field measurements have not detected evidence of this (Polashenski et al., 2015).

Stroeve (2001) analysed the Pathfinder surface albedo record, also from AVHRR observations, obtaining negative blue-sky albedo trends over a set of in situ measurement sites across the ice sheet during 1981-1998. The study noted, however, that the trends were not statistically significant and were largely driven by the anomalously low albedos observed during the summer of 1998, a feature present in CLARA as well. Yet our 1982-1999 subperiod sees few substantial albedo decreases apart from the northeastern and eastern margins. The difference to the earlier study is likely attributable to three factors. First, the CLARA record is based on a more sophisticated AVHRR intercalibration, and comprises of more satellites carrying the instrument relative to Pathfinder. Second, the Theil-Sen trend estimator used here is resistant against outlier influence in trends, such as that from the low-albedo summer of 1998. And thirdly, the Pathfinder albedo record quantified the blue-sky albedo of the ice sheet, thus containing an influence of variable cloud cover, whereas the CLARA record describes the black-sky albedo, which is an inherent property of the surface itself under unidirectional illumination.

We finally observe that some of the outermost grid cells of e.g. the western edge of the ice sheet display very small negative or even positive trends for all studied months. This finding, while somewhat surprising, is consistent with earlier field observations stating that the outermost zone of the ice sheet margin consists of clean ice, effectively drained of melt water by ubiquitous crevasses and moulins (Knap and Oerlemans, 1996) and containing fewer biotic or abiotic impurities, and thus resistant to albedo decreases caused by enhanced melting. However, we note that with the relatively coarse spatial resolution of CLARA, the outermost grid cells are mixed pixels even after the exclusion of grid cells with <50% ice cover. The albedo of these pixels includes relatively constant values of the bare soil surrounding the ice, which could also explain the observed stability. In any event, the impact of these areas on the overall ~~GrIS~~ ice sheet albedo trends is negligible~~ly small~~.

3.2. Melt intensity and bare ice exposure

~~The left column (S~~ubplots (a~~), d, h))~~ in Figure 4~~Figure 4~~ to Figure 6 show~~s~~ the change in the ~~mean albedo decrease rate~~time required from early May for the grid cell to reach an albedo typical of bare ice, taken as a proxy for melt season intensity, between the last and first 3 years of each period. Here, the decrease rates are shown only for elevations below 2200 m a.s.l., where the trend signal originates~~y are expected to be more robust~~. The overlaid pentagons (and crosses) indicate areas where albedos typical of bare ice and wet snow have been reached at the end but not the beginning of each period (and vice versa). The patterns correlate well spatially, as expected. We see increases in melt intensity along the western margin (Basin 5) for the full CLARA period and both subperiods~~, but t~~The MODIS era has seen systematically ~~faster albedo decrease rates also~~ more bare ice exposure also over Basin 6, further north. To assess the consistency and robustness of the changes in melt intensity, we also calculated the Theil-Sen decadal trend estimates for the melt rates during each period, shown in Figure

7~~Figure 5~~. The acceleration in melt rate between 1982 and 2015 is significant over large areas in the western, northern, and northeastern ~~GrIS~~ margins, largely as a consequence of a changes seen during 2000-2012.

Also, while some areas saw new bare ice exposure in the late 1990s (relative to early 1980s), there has been a widespread increase in areas experiencing bare ice exposure (or very wet snow cover) during the 2000s, so that these areas now routinely reach elevations 50 – 100 m higher up the ice sheet compared to 1982-1984 (Figure 8~~Figure 4a, inset~~). These changes are consistent with corresponding positive anomalies in MERRA-2 mean SAT during the summer months, as shown in Figure 4~~Figure 4~~ to Figure 6, subplots (c~~,f,j~~).

A notable and interesting deviation from this trend towards faster melt and expanding bare ice / very wet snow cover has occurred along the southeastern margin, roughly between Tasiilaq and Paamiut (Basin 4). Here, we observe no increase in melt rate during the MODIS era, and areas which reached bare ice albedos during the melting season at the turn of the century no longer do so in 2013-2015. We suggest that both of these effects are explained by substantial increases in winter snowfall over this region, as shown by the MERRA-2 winter precipitation anomalies (Figure 6~~Figure 4~~, subplot~~s~~ (b~~,e,i~~)). The increasing snow deposition, also reported by Box (2013), creates a buffer against melt rate acceleration, inhibiting bare ice exposure at the same time. The summer SAT anomalies during the MODIS era over this region are also less significant than those over the western margin, consistent with prior analysis suggesting that the presently dominant atmospheric circulation patterns particularly favour northward warm air transport along the western margin of the ice sheet (Fettweis et al., 2013), potentially enhanced at times by the so-called 'atmospheric river' events (Neff et al., 2014).

3.3. Runoff contribution in the variability of the ~~GrIS~~ ice sheet's Surface Mass Balance (SMB) ~~changes~~ in summer during ~~the past three decades~~1982-2015

Figure 9~~Figure 6a~~A shows the Theil-Sen regression fit between the monthly means of the CLARA albedo timeseries and the ~~GrIS~~ ice sheet SMB, obtained by correcting the GRACE mass balance observations with the state-of-the-art monthly ice discharge estimates (King et al., 2018) after eq. (1). The obtained fit shows no temporal dependency (years marked by colors ~~in Fig. 5a~~), and is fairly robust ($r^2 \sim 0.77$). For completeness, the regression parameters for both CLARA and MOD10A1 are provided in the supplementary material, and we discuss considerations and limitations to their use in section 2.7.4. ~~), and is of the form~~

~~$$SMB = 3028 \times \alpha_{CLARA-BSA} - 2222 \quad (3)$$~~

~~This sensitivity of SMB to albedo changes in this relationship, which we emphasize to be a statistical one, is markedly different between the CLARA-GRACE pair relative to the MOD10A1-GRACE pair, whose fit is less robust (r2 ~ 0.45) and reproduced here:~~

~~$$SMB = 1711 \times \alpha_{MODIS-BSA} - 1378 \quad (4)$$~~

Formatted: Normal, Left

Formatted: Normal, Left, Line spacing: single

~~Most of the difference is likely attributable to a substantially larger August mean GrIS albedo in MOD10A1 relative to CLARA. The MOD10A1 mean GrIS albedo is generally higher than in CLARA for any given month but this difference is most pronounced in August, likely due to different retrieval algorithms between the two products.~~

~~When applying the relationships of eq. (3) and eq. (4) to the respective MJJA albedo timeseries and summing to the summer SMB estimates, we obtain~~We then calculate the summer-summed proxy SMB for both CLARA and MOD10A1, ~~the results~~ shown in Figure 9~~Figure 6~~b. The original GRACE SMB estimates and ~~the calculated~~ MAR SMB are shown for comparison. Both proxy SMB timeseries overestimate MAR SMB, largely because the original GRACE SMB estimates do so as well. However, it is notable that the GRACE proxy SMB largely does agree with MAR SMB between 1982 and 2014 within its uncertainty envelope, apart from the a priori known period of 1992-1993, and 1999-2000 to a smaller extent. The 1999-2000 disagreement may be traceable to a change in the NOAA AVHRR constellation which occurred at the time. Both CLARA and MOD10A1 proxy SMB exhibit a significant Pearson correlation coefficient against MAR (CLARA: 0.79, MOD10A1: 0.95), ~~indicating that the proxies capture most of the annual variability in summer SMB~~confirming, on observational basis, the modeling-based finding that surface melt and subsequent runoff dominate the interannual summer SMB variability of the ice sheet.

A notable divergence between the proxies and MAR in the MODIS era occurs in 2012, when evidently the summer mass loss clearly outpaced any albedo reductions seen by either MODIS or AVHRR. A potential explanation is that albedo decreases are physically bounded in a way that the surface-melt induced mass loss is not. The albedo of the ice sheet margin, where the changes are concentrated, could be considered to have physically based local effective minima, corresponding to conditions where the ice sheet surface is consistently melting and saturated with melt ponds and melt rivers up to the local effective maximum coverage. In this logic, beyond this point the mean surface albedo of the area would have almost nowhere to go in terms of further decreases, barring the introduction of large concentrations of light-absorbing impurities or biomass.

~~Considering the completely independent nature of the proxy record sources in relation to each other (optical imagers vs. GRACE) on one hand, and between proxy observations and MAR model output on the other, the agreement seen in Figure 6B serves to first confirm the similarity of albedo reductions seen in MOD10A1 and CLARA, and also to implicitly confirm the dominant nature of runoff increase in the post-2000 rapid surface mass loss era (e.g. van den Broeke et al., 2016) on the other, as the albedo-based proxies can only be considered to be well-correlated to runoff in eq. (2). The general agreement of the CLARA proxy record with MAR within the AVHRR observational uncertainty also serves as an observation driven confirmation of the stability of SMB in the 1982-1999 period at the scale of the ice sheet.~~

Formatted: Font: 10 pt, Not Bold

3.4. On the basin-scale relationships between surface albedo as a runoff proxy, and ice discharge

A comparison between detrended, normalized basin-scale D anomalies and surface albedo (serving as a proxy for runoff) between 2000 and 2015 yielded no statistically significant relationships for any examined summer month at the 95% confidence level. This negative finding implies that surface runoff anomalies do not significantly alter the solid ice discharge rates through the ~~GrIS~~ outlet glaciers at the annual level. This is in line with previous modelling work (Schoof, 2010, Tedstone et al., 2015) which has suggested a complex relationship between meltwater availability and glacier flow rate, where large amounts of meltwater may serve to decelerate rather than accelerate glacier basal flow. Also, King et al. (2018) note that the annual variability in ~~GrIS~~ the ice discharge is mostly connected to cumulative changes in the calving front positions of its outlet glaciers.

~~However, Schoof (2010) as well as Tedstone et al. (2015) and King et al. (2018) note that short-term increases in meltwater runoff can temporarily increase basal water pressure, leading to glacier acceleration. This relationship is active in the early part of the melting season and typically operates at a narrow temporal window, with the current estimate for the temporal lag between fastest increase in runoff and the maximum GrIS D being 13 ± 9 days (King et al 2018). To examine this connection from observational evidence, we again adopted the surface albedo changes in CLARA-A2 SAL as a runoff proxy, and compare the timing of the maximum (detrended and normalized) D in each basin with the timing of fastest basin-scale albedo decrease, following the calculation outlined in section 2.7.3.~~

~~The thus obtained time lags (runoff proxy maximum minus D maximum) are shown in Figure 7. While year to year variability remains high, most of the years at most of the basins exhibit time lags within or similar to the expected time window. Temporal differences between maxima are largest in Basin 1, where there is generally more gradual sloping bed topography. By contrast, we note that temporal differences are smallest in the southeastern Basin 4, where glacier bed topographies are much steeper. The presence of negative time lags in the comparison also remind us that uncertainties still exist in the analysis, particularly in the determination of maximum runoff date from relatively noisy surface albedo data, even after statistical smoothing operations. Nevertheless, the close temporal proximity between maximum discharge and our observation-based runoff proxy in most basins suggest these two processes are dynamically related, supporting previous findings that runoff can influence glacier flow by altering subglacier water pressure and sliding speeds.~~

4. Discussion

The CLARA-A2 SAL surface albedo estimates are not normalized to any particular Sun Zenith Angle (SZA), but rather represent the per-grid cell mean solar illumination conditions of each 5-day or monthly time period. This choice is consciously made, as typically used SZA normalization algorithms (Briegleb et al., 1986; Gardner and Sharp, 2010) assume a noon-symmetrical 'u-shape' for the diurnal cycle of snow albedo. However, several in situ measurement campaigns have shown that

this choice is not valid for snow during the melting period, when the 'u-shape' is often noon-asymmetrical (Dirmhirn and Eaton, 1975; Jonsell et al., 2003; Pirazzini et al., 2006; Meinander et al., 2013). As here we study the ~~GrIS~~ ice sheet margins, where annual melting seasons are intensive, we have chosen not to present primary results based on an uncertain normalization procedure. For completeness, Supplementary Figure S1 reproduces Figure 3 with the application of the SZA normalization proposed by Gardner and Sharp (2010) with a target SZA of 60 degrees. The trends are consistent, demonstrating that the results shown here are not sensitive to the inclusion or exclusion of SZA normalization. Also, the separate treatment for each summer month and the use of a conservative SZA cutoff (of 70 degrees) in the albedo estimation will further ameliorate any ~~effects of this choice~~impacts of excluding a normalization procedure.

Regarding the recent inhibition of surface melt along the SE margin of the ice sheet, which we suggest is due to increasing winter precipitation, there are somewhat conflicting views in the recent literature. Berdahl et al. (2018) examined observation precipitation records at Tasiilaq station, taken to be representative of the surrounding parts of the SE ice sheet, and found no significant December-February precipitation increases in the satellite era up to 2012. However, Koyama and Stroeve (2018) evaluated the Arctic System Reanalysis precipitation against in situ observation along the ~~GrIS~~ ice sheet margins, and it is notable that in situ observations in their study indicated increasing precipitation in the 2010-2015 period at sites 04390 and 04272, near the southern tip of Greenland. These increases are in line with the increasing winter precipitation signal we observe in MERRA-2, and consistent with the lack of new albedo reductions or bare ice exposure in CLARA (Figure 6~~Figure 4~~~~Figure 4~~).

Wong et al. (2015) also reported consistent although regionally variable temperature and precipitation responses along the Greenland coastal regions to prevailing atmospheric circulation patterns, in particular to the warm and moist southerly air flows associated with a negative North Atlantic Oscillation (NAO) index. Their finding of increasing winter precipitation in the NW region of the ice sheet during 1990-2010 is consistent with the localized lack of systematic melt acceleration seen in CLARA over the same region (Figure 4), even though the increasing precipitation is not seen by MERRA-2. However, the reversal of bare ice exposure in the NW when comparing 2013-2015 to 2000-2002 (Figure 6) may also be related to more frequent cold northerly airflows post-2012 (Tedesco et al., 2014).

The curiously bimodal structure of the MERRA-2 winter precipitation anomalies between 2000-2015, with increases in the southernmost parts of the SE margins and reductions towards the east, is noteworthy but its deeper analysis is beyond the scope of this study. It is intriguing to note, however, that Tasiilaq station appears to lie at the no-change zone between the MERRA-2 bimodal peaks, which might serve to explain the lack of observed precipitation increases by Berdahl et al. (2018). Lastly, the efficacy of the melt inhibition depends fully on the phase of the precipitation; recent evidence ~~pointing towards an increasing replacement of snowfall with rainfall over southern GrIS may prove~~ demonstrates that the proportion of rainfall to total precipitation is increasing, suggesting that our finding ~~to~~ may be transient in nature (Oltmanns et al., 2019).

While our observation-based test confirms the dominance of surface melt in the surface mass loss of the ice sheet, ~~T~~the general agreement between modelled and ~~observation-based~~proxy SMB shown here contains substantial (though mutually cancelling) disagreements at the monthly level. Most notably, the ERA-Interim-forced MAR v.3.5.2~~.~~ SMB generally sees the largest annual mass loss occurring in July, whereas the corresponding GRACE SMB estimates assign the largest mass loss into the month of August. Such differences have emerged in prior studies (Alexander et al., 2016), although based on different GRACE mass balance solutions and a MAR version of different forcing and spatial resolution, invalidating direct comparisons between results. ~~A part of t~~The reasonably good covariability between MAR SMB and albedo-based proxy SMB is likely ~~also lies in~~ due, in part, to the ~~the better~~ improved agreement between GRACE and MAR mass balance at elevations below 2000 m a.s.l. (Alexander et al., 2016), where also most of the ~~GrIS~~ ice sheet albedo ~~dynamics occur~~changes occur. Also, in principle snowfall acts to increase both SMB and albedo, although the correlation is short-lived, diminishing once the fresh snow layer becomes optically semi-infinite.

The ESA Greenland Ice Sheet CCI distributes mass balance solutions from two algorithms (TUDresden and DTU). For completeness, we repeated the SMB analysis also for the DTU GRACE data. The results (Supplementary Figure S2) show a less favourable fit between CLARA and discharge-corrected GRACE SMB with a larger slope, leading to generally much less negative surface mass balance in the CLARA-GRACE proxy relative to MAR. The MOD10A1 is similarly affected but to a lesser degree. It is notable that both discharge-corrected GRACE SMB timeseries from ESA Greenland Ice Sheet CCI produce systematically less negative SMB during the summers 2004-2010 relative to MAR.

A variety of drivers of the post-2000 increases in ~~GrIS~~ the ice sheet's surface melt (and thus decreases in surface albedo) have been proposed. First are the atmospheric circulation pattern changes, which have led to warm and moist air advection over the ice sheet (e.g. Fettweis et al., 2013; Mioduszewski et al., 2016) leading to both increases in SAT (Reeves Eyre and Zeng, 2018) and increases in clear-sky downwelling longwave radiation (Mioduszewski et al., 2016; Välisuo et al., 2018). Another viewpoint has been that changes in the surface radiative energy budget, caused by cloud coverage and radiative property changes, are the primary driver. Hofer et al. (2017) argued, using the CLARA-A1 dataset, the predecessor of CLARA-A2 used here, that decreasing cloudiness over the ~~GrIS~~ ablation zone in the 2000s has caused a significant increase in insolation. This effect has combined with the increasing clear-sky downwelling longwave radiation from the warm air mass advection to cause the increasing melt. Along this theme but based on a different mechanism, Bennartz et al. (2013) argued that over the high-elevation center of the ice sheet, intrusions of optically thin, low-level, and liquid-bearing clouds drive the downward longwave flux up significantly, yet are thin enough to allow shortwave flux penetration to the surface, promoting extensive surface melt.

Here, we have focused on analysing the surface albedo changes using reanalysis SAT and winter precipitation as supporting evidence. For comparison purposes, we calculated the mean MJJA cloud fractional cover over ~~GrIS~~ the ice sheet from CLARA-

A2 (1982-2015) to compare against the corresponding MAR cloud cover field. The results in Figure 10~~Figure 8~~ show the change in CLARA cloud cover resulting from updated algorithms and AVHRR radiance calibration, resulting in a recovery of cloud cover after 2007 whereas MAR cloud cover continued to decline until 2011. This highlights the uncertainties in cloud observations from legacy AVHRR data, even though the detection performance has been shown to improve in CLARA-A2 (Karlsson et al., 2017)~~, with a~~A limited study over the central ~~GrIS~~ part of the accumulation zone during 2010 show~~ing~~ed good agreement between CLARA and MODIS cloud cover (Riihelä et al., 2017), implying that the latest years of CLARA with the highest number of concurrently serving AVHRR instruments should be the most reliable.

While the overall cloudiness decline from the mid-1990s to 2007 is still in line with the melt mechanisms proposed by Hofer et al. (2017), the post-2007 cloudiness recovery in CLARA-A2 is then inconsistent with the continuing large mass loss from the CLARA and MOD10A1 proxy SMB timeseries, as well as MAR, up till 2012. This suggests that the relationship between cloudiness, atmospheric circulation patterns, and surface melt ~~over GrIS~~ may be still more complicated than has been shown to date. Another complication lies in that not only the extent of cloud cover, but also its radiative properties, be they expressed through Cloud Optical Thickness (COT) and effective particle radius, or Liquid/Ice Water Path (LWP/IWP), are very important for correctly estimating the surface radiative energy budget over bright snow – and these retrievals from AVHRR are challenging (Riihelä et al., 2017).

Another means of linking large-scale atmospheric circulation to the surface albedo changes is via the Greenland Blocking Index (GBI; Hanna et al., 2013, 2016). Positive anomalies in GBI represent atmospheric conditions which block northerly zonal air flow over the ice sheet, allow for warm southerly air flow particularly across the west ~~GrIS~~ margin, and promote clear sky conditions over the ice sheet, enhancing surface melt (Hanna et al., 2014). The basin-scale comparisons between surface albedo anomalies and GBI anomalies (both calculated with respect to the 1982-2015 mean) are shown as time series in Figure 11~~Figure 9~~.

The negative correlation between GBI and albedo is evident (scatterplots available as Supplementary Figure S3), although different basins display different responses. For example, in agreement with Tedesco et al. (2016), the 2015 positive GBI anomaly was linked to an atmospheric ridge which enhanced melt in northern Greenland (basins 1 and 6) while preventing it in the south, a feature reproduced in the corresponding albedo anomalies. Along with the concurrent recovery in ~~GrIS~~ ice sheet mean cloudiness (Figure 10~~Figure 8~~), the significant ~~-~~covariability between GBI and albedo implies that the apparent post-2012 slowing in further albedo decreases is linked to a shift in large-scale atmospheric circulation, allowing for more cold northerly airflow (Tedesco et al., 2014) and increasing cloudiness (during summers; Figure 10).

McLeod and Mote (2016) also connect increasing surface melt since the early 1990s with the increasing frequency, and partly duration, of very large GBI (Greenland Blocking Episodes; GBE), in line with results from our observation-driven analysis.

Rajewicz and Marshall (2014) report that a substantial part of summer melt variability is directly explainable by increasing anticyclonic circulation over Greenland, isolating that signal from the overall near-surface air temperature increases and contesting that any abrupt change in atmospheric regime is behind the change. They also note that the anticyclonic circulation began to impact South Greenland already during the 1990s, with the effect spreading to other parts of the ice sheet after 2001. This is consistent with the gradually increasing albedo reduction seen in CLARA during the pre-MODIS era on the western margin, but does not explain the substantial late-summer albedo decrease in the Northeast in the same era.

The influence of oceanic heat advection is another possible cause for some of the observed albedo decreases. Both CLARA and MOD10A1 detect localized negative albedo trends around Helheim and Kangerdlussuaq glaciers in the southeast margin. Straneo et al. (2011) documented the presence of warm subtropical waters in the Helheim glacier fjord, and Häkkinen and Rhines (2009) showed that such waters have begun to penetrate the seas around SE Greenland with increasing intensity. It could thus be postulated that the release of heat from these warmer waters could act as a localized source of energy for the surface snow and ice for these two glaciers served by relatively large fjords.

Formatted: Font: Not Bold

Geolocation errors have been reported as a source of difference between the MODIS and AVHRR albedo estimates by Box et al. (2006). To further investigate the chance that geolocation and cloud masking uncertainties have a substantial impact on the obtained results, we compared the CLARA record to latest MOD10A1 (Box et al., 2017) in terms of decadal albedo trends and grid cell-specific mean differences per summer month during 2000-2015. The results are presented in the supplementary material (Supplementary Figure S4). The CLARA-MOD10A1 mean differences display a substantial latitudinal dependency in May and August, in line with results shown by Alexander et al. (2014). However, the decadal trends agree very well between the datasets, thus reinforcing the robustness of the observed trends in CLARA albedo. Discerning the cause of the differences would require a rigorous study accounting for differences in spatial resolution, diurnal sampling, and geolocation uncertainties, and is as such beyond the scope of the present work.

Finally, we note that while the CLARA proxy ~~offers a new look into period for which observation-based and spatially or temporally comprehensive estimates for SMB have been previously unavailable, the method shown has its limits. The SMB proxy may be derived only for the summer months when albedo retrievals are possible. Radiometric calibration and cloud detection uncertainties propagate into the surface albedo estimates as unwanted noise, which we have attempted to account for through an uncertainty envelope derived from a stability examination. Also,~~ does provide observation-based confirmation on the dominance of surface melt in the variability of the summed MJJA surface mass balance, the results show clear physical constraints on the validity of mechanisms linking enhanced albedo reductions as a proxy for SMB decreases. The question of increasing biological activity as a driver of albedo reduction along the ~~GrIS~~ ice sheet margins remains open and no long-term records exist for comparison with the present albedo estimates from CLARA. A large-scale spread of lichen colonies on the

ice surface would certainly provide a mechanism for albedo decrease unaccounted for in present models and satellite-based retrieval algorithms.

5. Conclusions

We have investigated the decadal trends in the surface albedo of the Greenland Ice Sheet between 1982 and 2015, and their connection to melt rate, bare ice exposure, as well as surface mass balance and ice discharge rate. The main results of this study may be summarized as follows.

- Over the 34-year investigation period, the late-summer surface albedo of the ~~GrIS~~ ice sheet margins shows statistically significant decrease at the 95% confidence level. The 1982-2015 decadal albedo trends reach a maximum of approximately -0.05 over the outermost ablation region in the Kangerlussuaq sector in July, although some grid cells in the area display decadal trends twice as large during 2000-2015. The trends are consistent with MODIS data for the overlap period.
- The albedo decrease of the northeastern and eastern margins was initiated during the 1982-1999 period, whereas the decrease along the west coast mainly occurred between 2000 and 2012, concurrently and consistently with a previously reported change in atmospheric circulation favouring the advection of warm and moist southerly airmasses along the west coast.
- The melt seasons along the western and northern ~~GrIS~~ ice sheet margins intensified after ~~the turn of the millennium~~2000, as seen by an acceleration of the albedo decrease rate during the melting season. Also, regions where surface melt causes the albedo to drop to values typical of bare ice were much more widespread in 2012-2015 than in the early 1980s, and expand to elevations 50-100 m higher on the ice sheet.
- A notable exception to the widespread albedo decrease was observed along the southern margins, where we propose that increased winter snowfall has created a buffer against snowmelt intensification and bare ice exposure. The future persistence of this effect will undoubtedly depend on the future magnitude and phase of precipitation along the ~~GrIS~~ ice sheet's southern margin.
- When calibrated against surface mass balance estimates based on GRACE gravimetric measurements and state-of-the-art ice discharge estimates, the CLARA surface albedo estimates form a proxy for summer-aggregated SMB reaching back to 1982. The ~~summer-only SMB~~ is proxy shows reasonably good agreement and a high degree of covariability with latest MAR regional climate model estimates for the full investigation period. This ~~indirectly~~ confirms the dominant role of surface runoff in ~~GrIS~~ the ice sheet's SMB variability during the satellite era~~, and highlights the sensitivity of albedo to surface runoff.~~
- We find no observational evidence for a connection between annual surface albedo changes (as a proxy for runoff production anomalies) and anomalies in annual rates of ice discharge at ~~GrIS~~ drainage basin-scales. This is in

agreement with recent modelling results which suggest that annual ice discharge is more sensitive to long-term variability in glacier front positions. ~~However, at shorter timescales, we find that the timings of maximum runoff production, estimated here as the period of fastest albedo decrease, and the seasonal maximum in normalized ice discharge generally exhibit time lags consistent with a previously reported range of 13 ± 9 days. These observations support a surface melt induced sliding mechanism, where surface melt waters that flow to the ice bed interface near the margins can temporarily increase basal water pressures and glacier sliding speeds.~~

Overall, the results fully fit into the present picture of ~~GrIS~~ the Greenland Ice Sheet being ~~an ice sheet~~ under duress, particularly between the mid-1990s and 2012. The decreasing albedo along the margins promotes enhanced surface melt, although atmospheric circulation patterns, cloud cover frequency and properties, as well as precipitation intensity and phase are most likely the strongest drivers of change manifested through surface mass loss and peripheral darkening of the ice sheet. Some of the albedo changes are also consistent with increasing biological activity in the surface ice as well as responses to ocean circulation changes, although the quantification of these links is beyond the scope of the present work. Albedo reductions along the ice sheet were ameliorated during ~~Years~~ 2013-2015 ~~show amelioration in the albedo decreases over GrIS margins~~, ~~yet~~ though the longevity of this feature remains to be seen.

Data availability

The CLARA-A2 surface albedo data record is available from https://doi.org/10.5676/EUM_SAF_CM/CLARA_AVHRR/V002. The MAR climate model data was obtained from ftp://ftp.climato.be/fettweis/MARv3.5/Greenland. The Greenland Ice Sheet CCI GRACE data was obtained from http://products.esa-icesheets-cci.org/products/downloadlist/GMB/. The Greenland Blocking Index was obtained from https://www.esrl.noaa.gov/psd/data/timeseries/daily/GBI/. The MOD10A1 albedo estimates were obtained from http://promice.dk/DownloadAlbedodata.html

Author contribution

A.R. planned the study and performed the analyses. M.K. was in charge of the discharge estimate data and contributed to the manuscript text. K.A. was the responsible scientist for the creation of the CLARA-A2 SAL dataset and contributed to the manuscript text. A.R. prepared the manuscript with contributions from all co-authors.

Competing interests

The authors declare that they have no conflict of interest.

Acknowledgments

The work of A.R. has been funded by the Academy of Finland, decision # 287399. Contributions from M.K. were supported by grants 80NSSC18K1027 and NN13AI21A from the US National Aeronautics and Space Administration.

The CLARA-A2 SAL data record was created by the Satellite Application Facility on Climate Monitoring (CM SAF), a project of EUMETSAT. Colleagues in the CM SAF project are thanked for their support in the creation of the CLARA-A2 SAL dataset. Supplementary Figures S1-S3 are available in the supporting information of this manuscript.

The authors would like to thank the editor, an anonymous reviewer and prof. Jason Box for their insight and comments that helped improve the manuscript.

Formatted: Normal, Line spacing: single

References

Alexander, P. M., Tedesco, M., Fettweis, X., Van De Wal, R., Smeets, C. J. P. P., & Van Den Broeke, M. R.: Assessing spatio-temporal variability and trends in modelled and measured Greenland Ice Sheet albedo (2000-2013). The Cryosphere, 8(6), 2293-2312, 2014.

Alexander, P. M., Tedesco, M., Schlegel, N.-J., Luthcke, S. B., Fettweis, X., ~~and~~ & Larour, E.: Greenland Ice Sheet seasonal and spatial mass variability from model simulations and GRACE (2003–2012), The Cryosphere, 10, 1259-1277, https://doi.org/10.5194/tc-10-1259-2016, 2016.

Anttila, K., Manninen, T., Jääskeläinen, E., & Riihelä, A.: Validation Report for CM SAF Cloud, Albedo, Radiation data record, AVHRR-based, Edition 2 (CLARA-A2) Surface Albedo. DOI: 10.5676/EUM_SAF_CM/CLARA_AVHRR/V002, 2016.

Barletta, V. R., Sørensen, L. S., ~~and~~ & Forsberg, R.: Scatter of mass changes estimates at basin scale for Greenland and Antarctica. The Cryosphere, 7(5), 1411–1432, 2013.

Bennartz, R., Shupe, M. D., Turner, D. D., Walden, V. P., Steffen, K., Cox, C. J., Kulie, M., Miller, B., & Pettersen, C.: July 2012 Greenland melt extent enhanced by low-level liquid clouds. Nature, 496(7443), 83, 2013.

Berdahl, M., Rennermalm, A., Hammann, A., Mioduszweski, J., Hameed, S., Tedesco, M., Stroeve, J., Mote, T., Koyama, T., & McConnell, J. R.: Southeast Greenland Winter Precipitation Strongly Linked to the Icelandic Low Position. Journal of Climate, 31(11), 4483-4500, 2018.

Bøggild, C. E., Brandt, R. E., Brown, K. J., & Warren, S. G.: The ablation zone in northeast Greenland: ice types, albedos and impurities. Journal of Glaciology, 56(195), 101-113, 2010.

Box, J. E., Bromwich, D. H., Veenhuis, B. A., Bai, L. S., Stroeve, J. C., Rogers, J. C., Steffen, K., Haran, T., & Wang, S. H.: Greenland ice sheet surface mass balance variability (1988–2004) from calibrated polar MM5 output. Journal of Climate, 19(12), 2783-2800, 2006.

Box, J. E., Fettweis, X., Stroeve, J. C., Tedesco, M., Hall, D. K., & Steffen, K.: Greenland ice sheet albedo feedback: thermodynamics and atmospheric drivers. The Cryosphere, 6(4), 821-839, 2012.

Box, J. E.: Greenland ice sheet mass balance reconstruction. Part II: Surface mass balance (1840–2010). Journal of Climate, 26(18), 6974-6989., 2013.

Box, J.E., Sharp, M., Aðalgeirsdóttir, G., Ananicheva, M., Andersen, M. L., Carr, R., Clason, C., Colgan, W., Copland, L., Glazovsky, A., Hubbard, A., Kjeldsen, K., Mernild, S., Moholdt, G., Moon, T., Wagner, T., Wouters, B., & Van Wychen, W.: Changes to Arctic land ice. In Snow, Water, Ice and Permafrost in the Arctic (SWIPA) 2017 (pp. 137-168). Oslo: Arctic Monitoring and Assessment Programme (AMAP), 2017.

Box, J.E., van As, D., & Steffen, K.: Greenland, Canadian and Icelandic land ice albedo grids (2000-2016), Geological Survey of Denmark and Greenland Bulletin, 38, 53-56, 2017.

Briegleb, B. P., Minnis, P., Ramanathan, V., ~~and~~ & Harrison, E.: Comparison of regional clear sky albedos inferred from satellite observations and model calculations, J. Clim. Appl. Meteorol., 25, 214– 226, 1986.

Casey, K. A., Polashenski, C. M., Chen, J., & Tedesco, M.: Impact of MODIS sensor calibration updates on Greenland Ice Sheet surface reflectance and albedo trends. The Cryosphere, 11(4), 1781-1795, 2017.

Citterio, M. ~~and~~ & Ahlstrøm, A. P.: Brief communication "The aerophotogrammetric map of Greenland ice masses", The Cryosphere, 7, 445-449, https://doi.org/10.5194/tc-7-445-2013, 2013.

Colgan, W., Box, J. E., Fausto, R. S., van As, D., Barletta, V. R., & Forsberg, R.: Surface albedo as a proxy for the mass balance of Greenland's terrestrial ice. Geol. Surv. Den. Greenl. Bull, 31, 91-94, 2014.

Cullather, R. I., Nowicki, S. M., Zhao, B., & Suarez, M. J.: Evaluation of the surface representation of the Greenland Ice Sheet in a general circulation model. Journal of Climate, 27(13), 4835-4856, 2014.

Dirmhirn, I., & Eaton, F. D.: Some characteristics of the albedo of snow. Journal of Applied Meteorology, 14(3), 375-379, 1975.

Enderlin, E. M., Howat, I. M., Jeong, S., Noh, M. J., van Angelen, J. H., & van den Broeke, M. R.: An improved mass budget for the Greenland ice sheet. Geophysical Research Letters, 41(3), 866-872, 2014.

Fearnhead, P.: Exact and efficient Bayesian inference for multiple changepoint problems. Statistics and computing, 16(2), 203-213, 2006.

Fettweis, X., Hanna, E., Lang, C., Belleflamme, A., Erpicum, M., & Gallée, H.: Important role of the mid-tropospheric atmospheric circulation in the recent surface melt increase over the Greenland ice sheet. The Cryosphere, 7, 241-248, 2013.

Fettweis, X., Box, J. E., Agosta, C., Amory, C., Kittel, C., Lang, C., van As, D., Machguth, H., ~~and~~ & Gallée, H.: Reconstructions of the 1900–2015 Greenland ice sheet surface mass balance using the regional climate MAR model, The Cryosphere, 11, 1015-1033, https://doi.org/10.5194/tc-11-1015-2017, 2017.

Forsberg, R., & Reeh, N.: Mass change of the Greenland Ice Sheet from GRACE. Gravity Field of the Earth – 1st meeting of the International Gravity Field Service. Springer Verlag, 2006. (IAG proceedings series).

Gardner, A. S., & Sharp, M. J.: A review of snow and ice albedo and the development of a new physically based broadband albedo parameterization. Journal of Geophysical Research: Earth Surface, 115(F1), 2010.

Gelaro, R., McCarty, W., Suárez, M. J., Todling, R., Molod, A., Takacs, L., Randles, C., Darmenov, A., Bosilovich, M., Reichle, R., Wargan, K., Coy, L., Cullather, R., Draper, C., Akalla, S., Buchard, V., Conaty, A., da Silva, A., Gu, W., Kim, G.-K., Koster, R., Lucchesi, R., Merkova, D., Nielsen, J., Partyka, G., Pawson, S., Putman, W., Rienecker, M., Schubert, S., Sienkiewitz, M., & Zhao, B.: The modern-era retrospective analysis for research and applications, version 2 (MERRA-2). Journal of Climate, 30(14), 5419-5454, 2017.

Groh, A., & Horwath, M.: The method of tailored sensitivity kernels for GRACE mass change estimates. Geophysical Research Abstracts, 18, EGU2016-12065, 2016.

Heidinger, A. K., Straka III, W. C., Molling, C. C., Sullivan, J. T., & Wu, X.: Deriving an inter-sensor consistent calibration for the AVHRR solar reflectance data record. International Journal of Remote Sensing, 31(24), 6493-6517, 2010.

Hall, D. K., Riggs, G. A., & Salomonson, V. V.: Development of methods for mapping global snow cover using moderate resolution imaging spectroradiometer data. Remote sensing of Environment, 54(2), 127-140, 1995.

Hanna, E., Jones, J. M., Cappelen, J., Mernild, S. H., Wood, L., Steffen, K., & Huybrechts, P.: The influence of North Atlantic atmospheric and oceanic forcing effects on 1900–2010 Greenland summer climate and ice melt/runoff. International Journal of Climatology, 33(4), 862-880, 2013.

Hanna, E., Fettweis, X., Mernild, S. H., Cappelen, J., Ribergaard, M. H., Shuman, C. A., Steffen, K., Wood, L., & Mote, T. L.: Atmospheric and oceanic climate forcing of the exceptional Greenland ice sheet surface melt in summer 2012. International Journal of Climatology, 34(4), 1022-1037, 2014.

Hanna, E., Cropper, T. E., Hall, R. J., & Cappelen, J.: Greenland Blocking Index 1851–2015: a regional climate change signal. International Journal of Climatology, 36(15), 4847-4861, 2016.

Helm, V., Humbert, A., & Miller, H.: Elevation and elevation change of Greenland and Antarctica derived from CryoSat-2. The Cryosphere, 8(4), 1539-1559, 2014.

Hofer, S., Tedstone, A. J., Fettweis, X., & Bamber, J. L.: Decreasing cloud cover drives the recent mass loss on the Greenland Ice Sheet. Science advances, 3(6), e1700584, 2017.

Hakkinen, S., & Rhines, P. B.: Shifting surface currents in the northern North Atlantic Ocean. Journal of Geophysical Research: Oceans, 114(C4), 2009.

Jonsell, U., Hock, R., & Holmgren, B.: Spatial and temporal variations in albedo on Storglaciären, Sweden. Journal of Glaciology, 49(164), 59-68, 2003.

Formatted: English (United States)

Jääskeläinen, E., Manninen, T., Tamminen, J., & Laine, M.: The Aerosol Index and Land Cover Class Based Atmospheric Correction Aerosol Optical Depth Time Series 1982–2014 for the SMAC Algorithm. Remote Sensing, 9(11), 1095, 2017.

Joughin, I., Smith, B. E., Howat, I. M., Floricioiu, D., Alley, R. B., Truffer, M., & Fahnestock, M.: Seasonal to decadal scale variations in the surface velocity of Jakobshavn Isbrae, Greenland: Observation and model-based analysis. Journal of Geophysical Research: Earth Surface, 117(F2), 2012.

Karlsson, K.-G., Anttila, K., Trentmann, J., Stengel, M., Fokke Meirink, J., Devasthale, A., Hanschmann, T., Kothe, S., Jääskeläinen, E., Sedlar, J., Benas, N., van Zadelhoff, G.-J., Schlundt, C., Stein, D., Finkensieper, S., Håkansson, N., ~~and~~ & Hollmann, R.: CLARA-A2: the second edition of the CM SAF cloud and radiation data record from 34 years of global AVHRR data, Atmos. Chem. Phys., 17, 5809-5828, https://doi.org/10.5194/acp-17-5809-2017, 2017.

King, M. D., Howat, I. M., Jeong, S., Noh, M. J., Wouters, B., Noël, B., & Broeke, M. R.: Seasonal to decadal variability in ice discharge from the Greenland ice sheet. The Cryosphere, 12(12), 3813-3825, 2018.

Knap, W. H., & Oerlemans, J.: The surface albedo of the Greenland ice sheet: satellite-derived and in situ measurements in the Søndre Strømfjord area during the 1991 melt season. Journal of Glaciology, 42(141), 364-374, 1996.

Konzelmann, T., & Braithwaite, R. J.: Variations of ablation, albedo and energy balance at the margin of the Greenland ice sheet, Kronprins Christian Land, eastern north Greenland. Journal of Glaciology, 41(137), 174-182, 1995.

Koyama, T., & Stroeve, J.: Greenland monthly precipitation analysis from the Arctic System Reanalysis (ASR): 2000–2012. Polar Science, 2018.

Mayer-Gürr, T., Behzadpour, S., Ellmer, M., Kvas, A., Klinger, B., & Zehentner, N.: ITSG-Grace2016 - Monthly and Daily Gravity Field Solutions from GRACE. GFZ Data Services. http://doi.org/10.5880/icgem.2016.007, 2016.

McLeod, J. T., & Mote, T. L.: Linking interannual variability in extreme Greenland blocking episodes to the recent increase in summer melting across the Greenland ice sheet. International Journal of Climatology, 36(3), 1484-1499, 2016.

Meinander, O., Kazadzis, S., Arola, A., Riihelä, A., Räisänen, P., Kivi, R., Kontu, A., Kouznetsov, R., Sofiev, M., Svensson, J., Suokanerva, H., Aaltonen, V., Manninen, T., Roujean, J.-L., & Hautecoeur, O..: Spectral albedo of seasonal snow during intensive melt period at Sodankylä, beyond the Arctic Circle. Atmospheric Chemistry and Physics, 13(7), 3793-3810, 2013.

Mernild, S. H., Hanna, E., McConnell, J. R., Sigl, M., Beckerman, A. P., Yde, J. C., Cappelen, J., Malmros, J. & Steffen, K.: Greenland precipitation trends in a long-term instrumental climate context (1890–2012): evaluation of coastal and ice core records. International Journal of Climatology, 35(2), 303-320, 2015.

Mioduszewski, J. R., Rennermalm, A. K., Hammann, A., Tedesco, M., Noble, E. U., Stroeve, J. C., & Mote, T. L.: Atmospheric drivers of Greenland surface melt revealed by self-organizing maps. Journal of Geophysical Research: Atmospheres, 121(10), 5095-5114, 2016.

Mouginot, J., Rignot, E., Scheuchl, B., Fenty, I., Khazendar, A., Morlighem, M., Buzzi, A., & Paden, J.: Fast retreat of Zachariæ Isstrøm, northeast Greenland. Science, 350(6266), 1357-1361, 2015.

Moustafa, S. E., Rennermalm, A. K., Román, M. O., Wang, Z., Schaaf, C. B., Smith, L. C., Koenig, L., & Erb, A.: Evaluation of satellite remote sensing albedo retrievals over the ablation area of the southwestern Greenland ice sheet. Remote sensing of environment, 198, 115-125, 2017.

Neff, W., Compo, G. P., Martin Ralph, F., & Shupe, M. D.: Continental heat anomalies and the extreme melting of the Greenland ice surface in 2012 and 1889. Journal of Geophysical Research: Atmospheres, 119(11), 6520-6536, 2014.

Oltmanns, M., Straneo, F., and Tedesco, M.: Increased Greenland melt triggered by large-scale, year-round cyclonic moisture intrusions, The Cryosphere, 13, 815-825, https://doi.org/10.5194/tc-13-815-2019, 2019.

Polashenski, C. M., Dibb, J. E., Flanner, M. G., Chen, J. Y., Courville, Z. R., Lai, A. M., Schauer, J., Shafer, M., & Bergin, M.: Neither dust nor black carbon causing apparent albedo decline in Greenland's dry snow zone: Implications for MODIS C5 surface reflectance. Geophysical Research Letters, 42(21), 9319-9327, 2015.

Rajewicz, J., & Marshall, S. J.: Variability and trends in anticyclonic circulation over the Greenland ice sheet, 1948–2013. Geophysical Research Letters, 41(8), 2842-2850, 2014.

Reeves Eyre, J. E., & Zeng, X.: Evaluation of Greenland near surface air temperature datasets. The Cryosphere, 11(4), 1591-1605, 2017.

Riihelä, A., Manninen, T., Laine, V., Andersson, K., & Kaspar, F.: CLARA-SAL: a global 28 yr timeseries of Earth's black-sky surface albedo. Atmospheric Chemistry and Physics, 13(7), 3743-3762, 2013.

Riihelä, A., Key, J. R., Meirink, J. F., Kuipers Munneke, P., Palo, T., & Karlsson, K. G.: An intercomparison and validation of satellite-based surface radiative energy flux estimates over the Arctic. Journal of Geophysical Research: Atmospheres, 122(9), 4829-4848, 2017.

Ryan, J. C., Hubbard, A., Stibal, M., Irvine-Fynn, T. D., Cook, J., Smith, L. C., Cameron, K., & Box, J.: Dark zone of the Greenland Ice Sheet controlled by distributed biologically-active impurities. Nature communications, 9(1), 1065, 2018.

Sasgen, I., van den Broeke, M., Bamber, J. L., Rignot, E., Sørensen, L. S., Wouters, B., Martinec, Z., Velicogna, I., & Simonsen, S. B.: Timing and origin of recent regional ice-mass loss in Greenland. Earth and Planetary Science Letters, 333, 293-303, 2012.

Schaaf, C. B., Gao, F., Strahler, A. H., Lucht, W., Li, X., Tsang, T., Strugnell, N., Zhang, X., Jin, Y., Muller, J-P., Lewis, P., Barnsley, M., Hobson, P., Disney, M., Roberts, G., Dunderdale, M., Doll, C., d'Entremont, R., Hu, B., Liang, S., Privette, J. & Roy, D.: First operational BRDF, albedo nadir reflectance products from MODIS. Remote sensing of Environment, 83(1-2), 135-148, 2002.

Schoof, C.: Ice-sheet acceleration driven by melt supply variability. Nature, 468(7325), 803, 2010.

Sen, P. K.: Estimates of the Regression Coefficient Based on Kendall's Tau. Journal of the American Statistical Association, 63: 1379–1389, 1968.

Sørensen, L. S. and Forsberg, R.: Greenland ice sheet mass loss from GRACE monthly models, gravity, Geoid Earth Obs., 135, 527–532, doi:10.1007/978-3-642-10634-7_70, 2010.

Stearns, L. A., & van der Veen, C. J.: Friction at the bed does not control fast glacier flow. Science, 361(6399), 273-277, 2018.

Straneo, F., Curry, R. G., Sutherland, D. A., Hamilton, G. S., Cenedese, C., Våge, K., & Stearns, L. A.: Impact of fjord dynamics and glacial runoff on the circulation near Helheim Glacier. Nature Geoscience, 4(5), 322, 2011.

Stroeve, J., Box, J. E., Wang, Z., Schaaf, C., & Barrett, A.: Re-evaluation of MODIS MCD43 Greenland albedo accuracy and trends. Remote sensing of environment, 138, 199-214, 2013.

Tedesco, M., Fettweis, X., Van den Broeke, M. R., Van de Wal, R. S. W., Smeets, C. J. P. P., van de Berg, W. J., Serreze, M., & Box, J. E.: The role of albedo and accumulation in the 2010 melting record in Greenland. Environmental Research Letters, 6(1), 014005, 2011.

Tedesco, M., J.E. Box, J. Cappelen, X. Fettweis, T.S. Jensen, T. Mote, A.K. Rennermalm, L.C. Smith, R.S.W. van de Wal and J. Wahr: Greenland Ice Sheet [in "State of the Climate in 2013"]. Bulletin of the American Meteorological Society, 95:S5-49, 2014.

Tedesco, M., Mote, T., Fettweis, X., Hanna, E., Jeyaratnam, J., Booth, J. F., Datta, R., & Briggs, K.: Arctic cut-off high drives the poleward shift of a new Greenland melting record. Nature communications, 7, 11723, 2016.

Tedstone, A. J., Nienow, P. W., Gourmelen, N., Dehecq, A., Goldberg, D., & Hanna, E.: Decadal slowdown of a land-terminating sector of the Greenland Ice Sheet despite warming. Nature, 526(7575), 692, 2015.

Tedstone, A. J., Bamber, J. L., Cook, J. M., Williamson, C. J., Fettweis, X., Hodson, A. J., & Tranter, M.: Dark ice dynamics of the south-west Greenland Ice Sheet. The Cryosphere, 11(6), 2491-2506, 2017.

Theil, H.: A rank-invariant method of linear and polynominal regression analysis (Parts 1-3). In Ned. Akad. Wetensch. Proc. Ser. A (Vol. 53, pp. 1397-1412), 1950.

van den Broeke, M., Enderlin, E. M., Howat, I. M., Kuipers Munneke, P., Noël, B. P., van de Berg, W., van Meijgaard, E. & Wouters, B.: On the recent contribution of the Greenland ice sheet to sea level change. The Cryosphere, 10(5), 1933-1946, 2016.

van den Broeke, M., Box, J., Fettweis, X., Hanna, E., Noël, B., Tedesco, M., van As, D., van de Berg, W., & van Kampenhout, L.: Greenland ice sheet surface mass Loss: recent developments in observation and modeling. Current Climate Change Reports, 3(4), 345-356, 2017

van den Broeke, M., Bus, C., Ettema, J., & Smeets, P.: Temperature thresholds for degree-day modelling of Greenland ice sheet melt rates. Geophysical Research Letters, 37(18), 2010.

Välisuo, I., Vihma, T., Pirazzini, R., & Schäfer, M.: Interannual Variability of Atmospheric Conditions and Surface Melt in Greenland in 2000–2014. Journal of Geophysical Research: Atmospheres, 123(18), 10-443, 2018.

Wong, G. J., Osterberg, E. C., Hawley, R. L., Courville, Z. R., Ferris, D. G., & Howley, J. A.: Coast-to-interior gradient in recent northwest Greenland precipitation trends (1952–2012). Environmental Research Letters, 10(11), 114008, 2015.

Xiong, X., Stamnes, K. and Lubin D.: Surface albedo over the Arctic Ocean derived from AVHRR and its validation with SHEBA data. Journal of Applied Meteorology, 41, 413–425, 2002.

Xuan, X., & Murphy, K.: Modeling changing dependency structure in multivariate time series. In Proceedings of the 24th international conference on Machine learning (pp. 1055-1062). ACM, 2007.

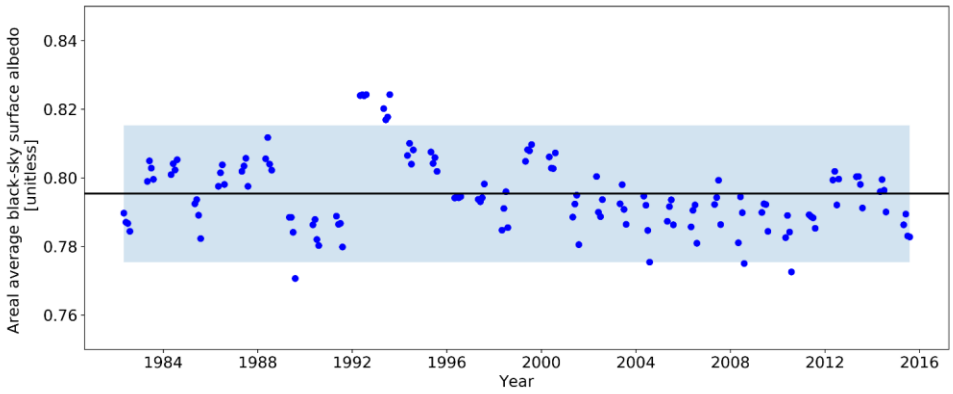

Figure 1: Stability of CLARA-A2 SAL over 73-75 °N, 38-42 °W, on the central part of ~~G-IS~~the Greenland ice sheet. Spatially averaged monthly mean albedo retrievals between May and August shown. The black line shows the 34-yr mean albedo of the area. Light blue shading shows ±0.02 albedo variability about the interannual mean, corresponding to the reported upper accuracy estimate of 5% relative for CLARA-A2 SAL over snow and ice.

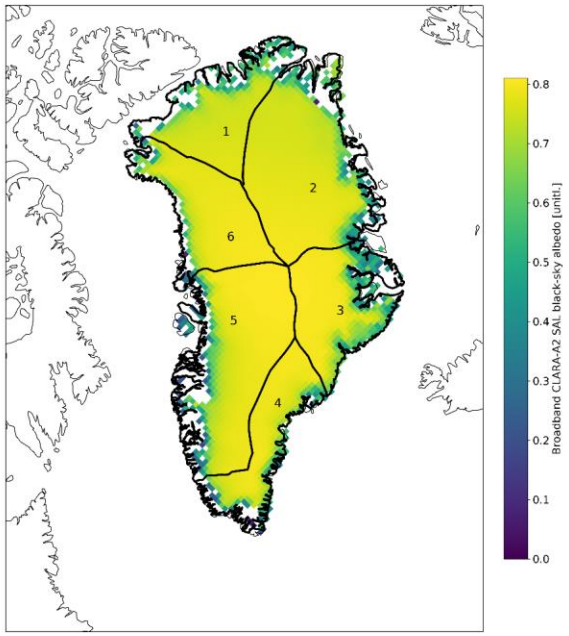

Figure 2: ~~GrIS~~ Ice sheet drainage basins as used in this study. Basin boundaries overlaid on an example of CLARA-A2 SAL monthly mean surface albedo from June 2010.

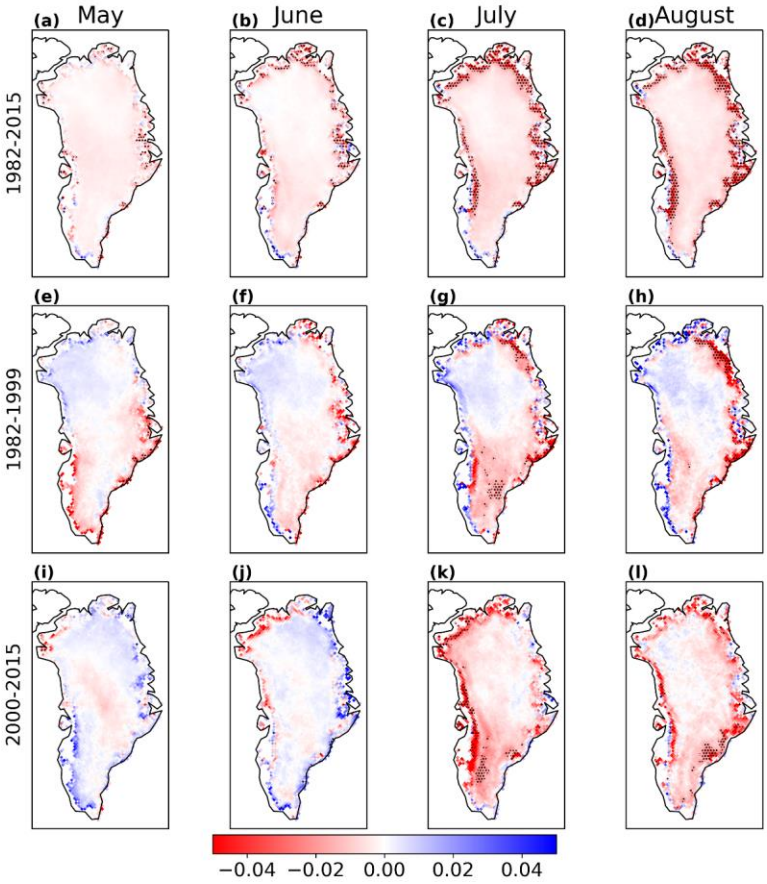

Figure 3: Theil-Sen decadal albedo trends over ~~GrIS~~ the ice sheet from CLARA-A2 SAL during 1982-2015 (a-d), 1982-1999 (e-~~h~~), and 2000-2015 (~~i~~j-~~l~~m). Columns correspond to the summer months May-August from left to right. The hatched regions in the trend figures indicate areas over which the trend is significant (i.e. non-zero slope) at the 95% confidence level, and its magnitude exceeds the uncertainty limit of 0.015/decade. Years 1992 and 1993 are excluded. Color bar limited to highlight majority values.

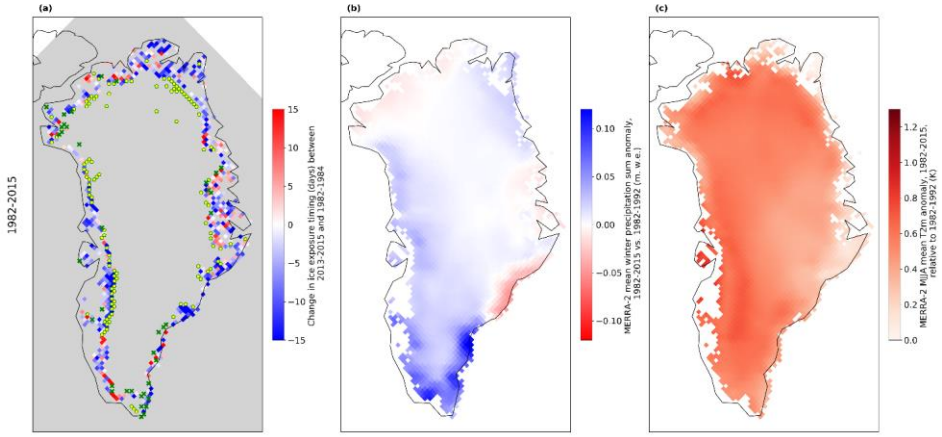

Figure 4: ~~Subplots~~ (a~~,d,h~~): ~~Estimated mean albedo decrease rate c~~Changes in time required (days) to reach bare ice-typical albedos between averaged periods ~~the last three and first three years~~ 2013-2015 and ~~of each analysed period~~1982-1984. Green-yellow pentagons indicate areas where bare ice albedo is reached during the last but not the first years of the period. Crosses indicate vice versa. ~~Subplots~~ (b~~,e,i~~): MERRA-2 mean winter precipitation anomaly [m w.e.] of ~~each period~~1982-2015 vs. 1982-1992 mean. ~~Subplots~~ (c~~,f,j~~): MERRA-2 mean May-August SAT anomaly of ~~each period~~ 1982-2015 vs. 1982-1999 mean.

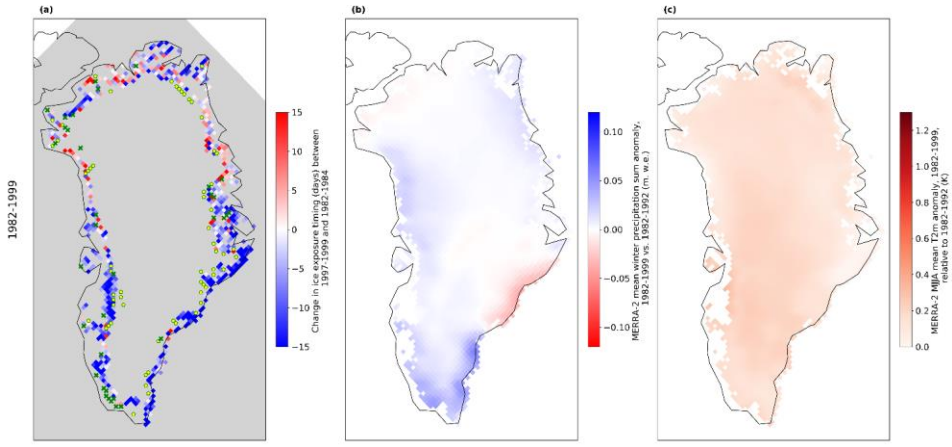

Figure 5: (a): Changes in time required (days) to reach bare ice-typical albedos between averaged periods 1997-1999 and 1982-1984. Green-yellow pentagons indicate areas where bare ice albedo is reached during the last but not the first years of the period. Crosses

Formatted: Keep with next

indicate vice versa. (b): MERRA-2 mean winter precipitation anomaly [m w.e.] of 1982-1999 vs. 1982-1992 mean. (c): MERRA-2 mean May-August SAT anomaly of 1982-1999 vs. 1982-1999 mean.

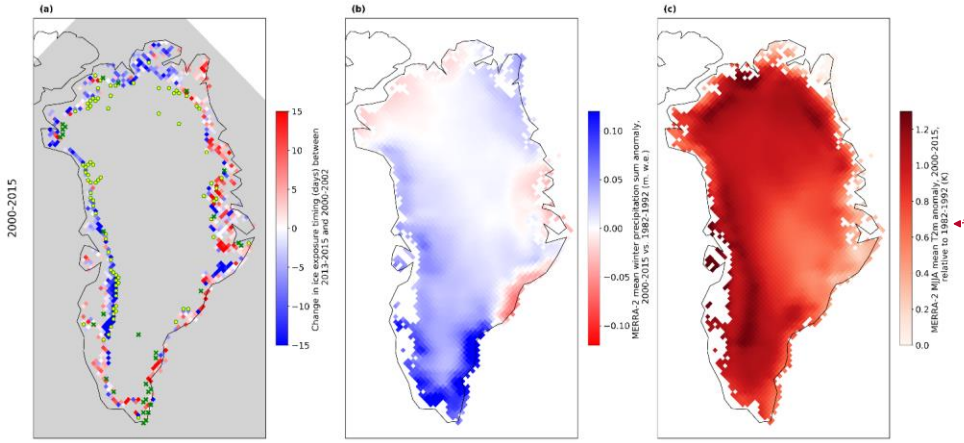

Figure 6: (a): Changes in time required (days) to reach bare ice-typical albedos between averaged periods 2013-2015 and 2000-2002. Green-yellow pentagons indicate areas where bare ice albedo is reached during the last but not the first years of the period. Crosses indicate vice versa. (b): MERRA-2 mean winter precipitation anomaly [m w.e.] of 1982-1999 vs. 1982-1992 mean. (c): MERRA-2 mean May-August SAT anomaly of 1982-1999 vs. 1982-1999 mean.

~~Period rows ordered as in Figure 3.~~

Formatted: Keep with next

Formatted: Normal

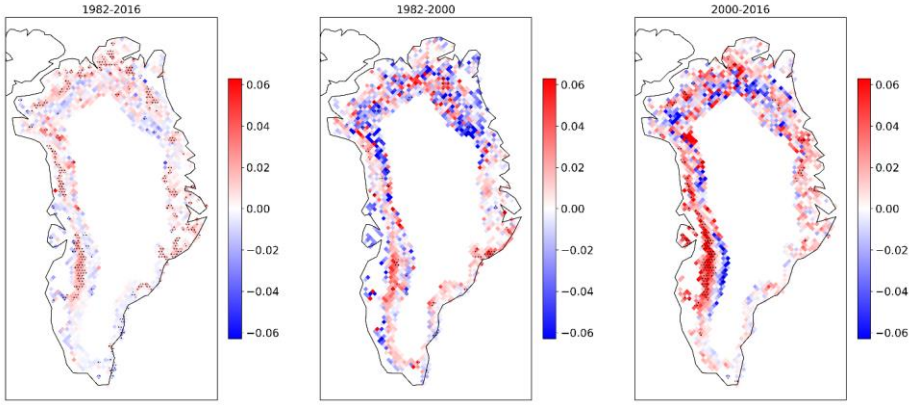

Figure 7~~5~~: Theil-Sen decadal trend estimates in albedo decrease rate [units per 30 days] serving as a proxy for melt intensity. Hatched pattern indicates areas where the trend is statistically significant (non-zero slope) at the 95% confidence level. Estimates shown only for elevations lower than 2200 m a.s.l.

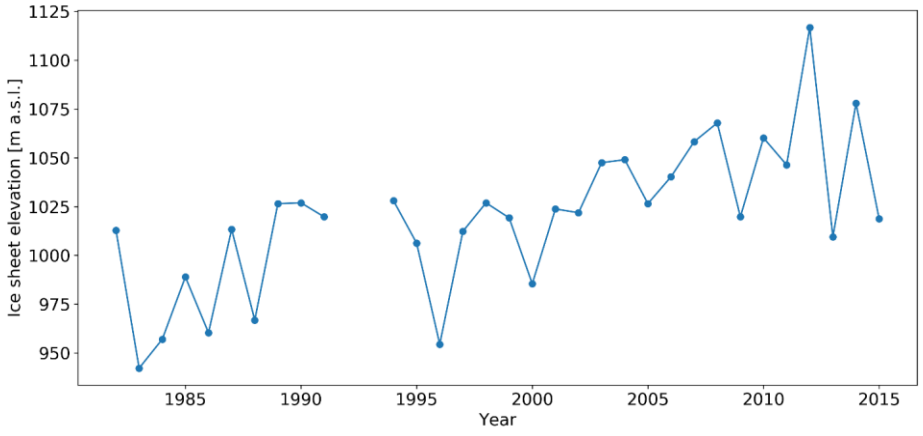

Figure 8: Change in the median elevation (a.s.l.) of the parts of the ice sheet reaching albedo typical of bare ice between 1982 and 2015. Years 1992 and 1993 excluded from analysis.

Formatted: Normal

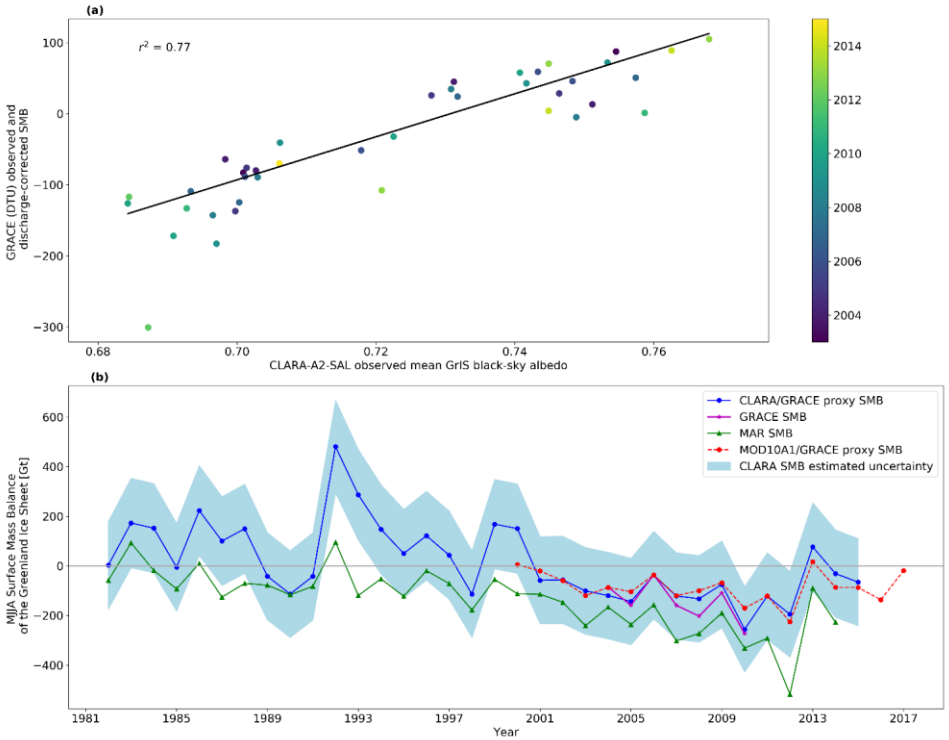

Figure 96: (a) Linear regression fit between CLARA-A2 SAL monthly mean ~~GrIS~~ ice sheet surface albedo (x-axis) and the TUDresden GRACE RL06 monthly SMB, obtained by correcting the GRACE mass balance data with ice discharge estimates by King et al. (2018). (b) ~~GrIS~~ May-August (MJJA) surface mass balance sums between 1982 and 2017. Blue line and markers show the CLARA-proxy SMB as calibrated against GRACE observations, with uncertainty envelope (blue shading) based on best-estimate for ~~GrIS~~ the mean snow/ice albedo stability of 0.02 in CLARA. Green line shows the corresponding SMB estimates from the MAR regional climate model. The magenta line and markers show the discharge-corrected GRACE SMB estimate, shown only for years with full GRACE MJJA availability. The red dashed line and markers show the MOD10A1-based SMB estimate for comparison.

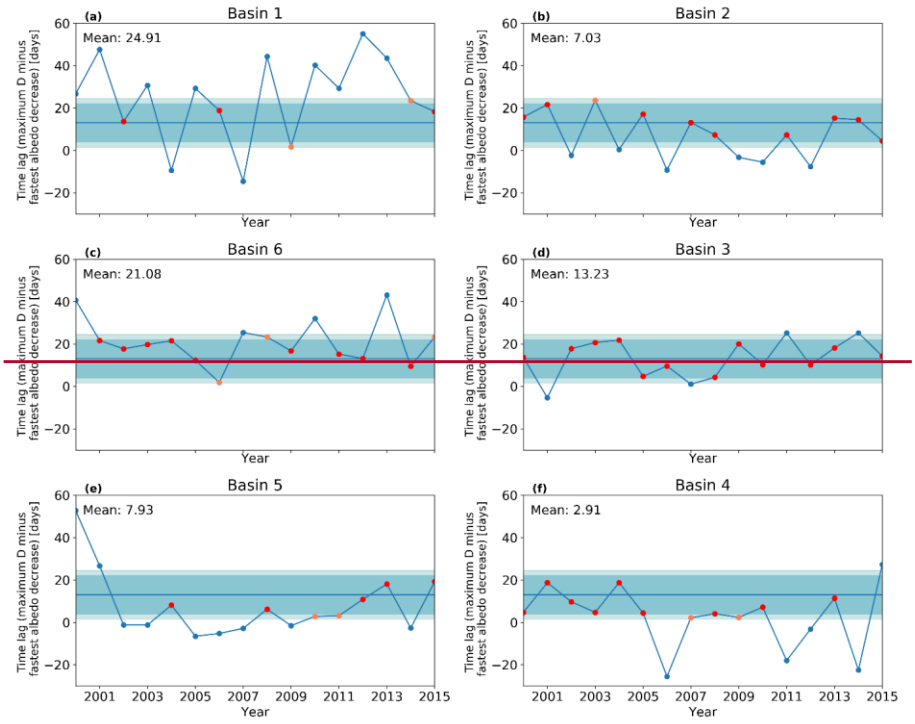

~~Figure 7: Basin-averaged annual time lags between maximum runoff production, obtained by proxy from each basin's surface albedo timeseries, and the annual maximum in solid ice discharge (D), obtained from normalized basin-scale discharge rates by King et al. (2018). Blue shaded region illustrates the expected time lag window of 13 ± 9 days from modelling (King et al., 2018). Light blue shading represents the additional temporal uncertainty related to the five-day temporal resolution in the source data. Red (and pink) markers indicate years in which the time lag agrees with the expected range (or with the additional uncertainty taken into account). Note that basins are ordered here by their relative geographical position.~~

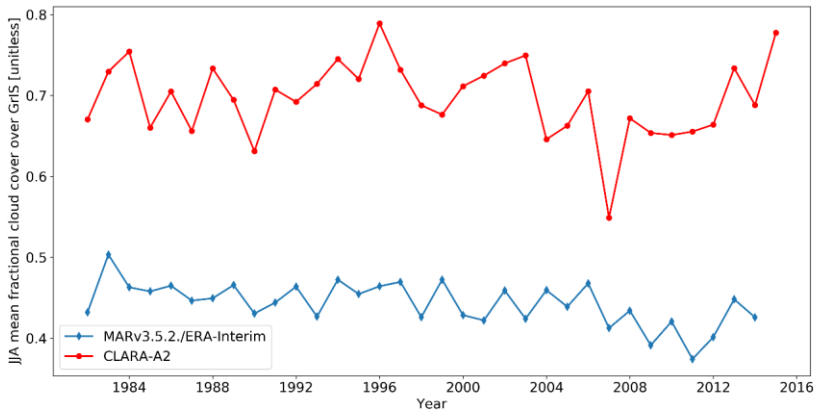

Figure 108: Mean JJA fractional cloud cover over ~~GrIS~~ the ice sheet from CLARA-A2 and MAR v3.5.2 with ERA-Interim forcing.

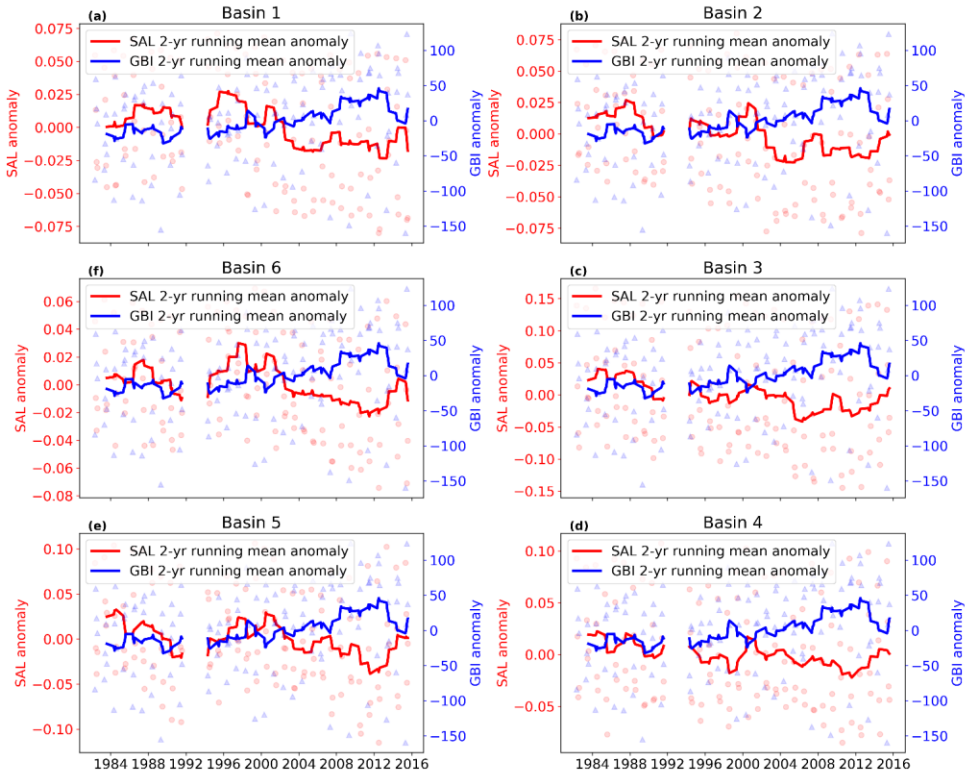

Figure 119: Comparison of monthly basin-scale CLARA-A2 SAL anomalies (red circle) against Greenland Blocking Index (GBI) anomalies (blue triangle). All anomalies calculated with respect to the 1982-2015 mean albedo or GBI. Red and blue lines show 2-year running means of the respective anomalies. Basins ordered as in Figure 2~~Figure 7~~. Years 1992 and 1993 excluded from the analysis.

Field Code Changed